



**MATHEMATICAL MODELLING OF HEAT AND MASS  
TRANSFER ON BIO-COAL PELLETS IN THE COMBUSTION  
PROCESS**

**BY**

**MISS MANUNCHAYA NOOWATTANA**

**A THESIS SUBMITTED IN PARTIAL FULFILLMENT OF THE  
REQUIREMENTS FOR THE DEGREE OF  
MASTER OF SCIENCE (MATHEMATICS)  
DEPARTMENT OF MATHEMATICS AND STATISTICS  
FACULTY OF SCIENCE AND TECHNOLOGY  
THAMMASAT UNIVERSITY  
ACADEMIC YEAR 2015  
COPYRIGHT OF THAMMASAT UNIVERSITY**

**MATHEMATICAL MODELLING OF HEAT AND MASS  
TRANSFER ON BIO-COAL PELLETS IN THE COMBUSTION  
PROCESS**

**BY**

**MISS MANUNCHAYA NOOWATTANA**

**A THESIS SUBMITTED IN PARTIAL FULFILLMENT OF THE  
REQUIREMENTS FOR THE DEGREE OF  
MASTER OF SCIENCE (MATHEMATICS)  
DEPARTMENT OF MATHEMATICS AND STATISTICS  
FACULTY OF SCIENCE AND TECHNOLOGY  
THAMMASAT UNIVERSITY  
ACADEMIC YEAR 2015  
COPYRIGHT OF THAMMASAT UNIVERSITY**



THAMMASAT UNIVERSITY  
FACULTY OF SCIENCE AND TECHNOLOGY  
THESIS

BY  
MISS MANUNCHAYA NOOWATTANA

ENTITLED

MATHEMATICAL MODELLING OF HEAT AND MASS TRANSFER ON  
BIO-COAL PELLETS IN THE COMBUSTION PROCESS

was approved as partial fulfillment of the requirements for  
the degree of Master of Science (Mathematics)

on July 8, 2016

Chairman

Sittipong Ruktamatakul  
(Assistant Professor Sittipong Ruktamatakul, Ph.D.)

Member and Advisor

S. KONGNUAN  
(Assistant Professor Supachara Kongnuan, Ph.D.)

Member

Ekkachai K.  
(Ekkachai Kunawuttipreechachan, Ph.D.)

Member

Khajee Jantarakhajorn  
(Khajee Jantarakhajorn, Ph.D.)

Member

Saifon Chaturantabut  
(Saifon Chaturantabut, Ph.D.)

Dean

P. Sermsuk  
(Associate Professor Pakorn Sermsuk)

Thesis Title	Mathematical Modelling of Heat and Mass Transfer on Bio-Coal Pellets in the Combustion Process
Author	Miss Manunchaya Noowattana
Degree	Master of Science in Mathematics
Department/Faculty/University	Department of Mathematics and Statistics Faculty of Science and Technology Thammasat University
Thesis Advisor	Supachara Kongnuan, Ph.D.
Academic Year	2015

### ABSTRACT

In this research, two models have been developed to study the distribution of heat and mass transfer and boundary movement in the combustion process of a bio-coal pellet. The models are considered on a bio-coal in a cylindrical shape which is burned only one side. One of the models, heat and mass transfer inside the particle are described by the governing equations including the heat transfer equation couple with the mass balance equation in transient state with appropriate initial and boundary conditions. Moreover, the parameters, thermal conductivity and specific heat capacity of several materials, are investigated to observe the behavior of heat and mass transfer. Another model describes heat and mass transfer with boundary movement of a bio-coal in the combustion process by using the Arbitrary Lagrangian Eulerian (ALE) technique. In this study, numerical simulation of heat and mass transfer and moving boundary of bio-coal pellets in the combustion process are presented by using algorithm based on the finite element method in the commercial software of COMSOL Multiphysics. The numerical results are feasible, reasonable and good agreement with previous studies which can be useful to develop qualities of bio-coal.

**Keywords:** bio-coal pellet, heat transfer, mass transfer, combustion, boundary movement.

## ACKNOWLEDGEMENTS

I would like to express my deepest appreciation to my thesis advisor, Asst.Prof.Dr. Supachara Kongnuan for her guidance, kindness, and encouragement throughout the course of this research. All her advice and teaching have been of great value to me in preparation of this thesis. In addition, I am grateful to her for the giving consultation on the issue and always supporting me.

I would like to thank my master committee members: Asst.Prof.Dr. Sittipong Ruktamatakul, Dr. Ekkachai Kunawuttipreechachan, Dr. Khajee Jantarakhajorn and Dr. Saifon Chaturantabut. Their suggestions and insightful comments very useful to improve my thesis.

I would like to thank Department of Mechanical Engineering, Thammasat University for the commercial software, COMSOL Multiphysics support.

I also wish to thank the Department of Mathematics and Statistics, Thammasat University for providing me with the necessary facilities.

Finally, I am very grateful to my family for their encouragement and all support.

Manunchaya Noowattana

# CONTENTS

<b>ABSTRACT</b>	<b>i</b>
<b>ACKNOWLEDGEMENTS</b>	<b>ii</b>
<b>TABLE OF CONTENTS</b>	<b>iv</b>
<b>LIST OF FIGURES</b>	<b>v</b>
<b>1 INTRODUCTION</b>	<b>1</b>
1.1 Heat and Mass Transfer . . . . .	3
1.2 The Combustion Process . . . . .	4
1.3 Scope and Objectives of the Research . . . . .	5
1.4 Outline of the Thesis . . . . .	6
<b>2 LITERATURE REVIEWS</b>	<b>7</b>
2.1 Heat and Mass Transfer . . . . .	7
2.2 Moving Boundary . . . . .	21
<b>3 HEAT AND MASS TRANSFER OF BIO-COAL PELLETS IN THE COM- BUSTION PROCESS</b>	<b>27</b>
3.1 General Overview . . . . .	27
3.2 Model Formulation . . . . .	29
3.3 Method of Solution . . . . .	33
3.4 Numerical Results and Discussion . . . . .	34
3.5 Conclusion . . . . .	42

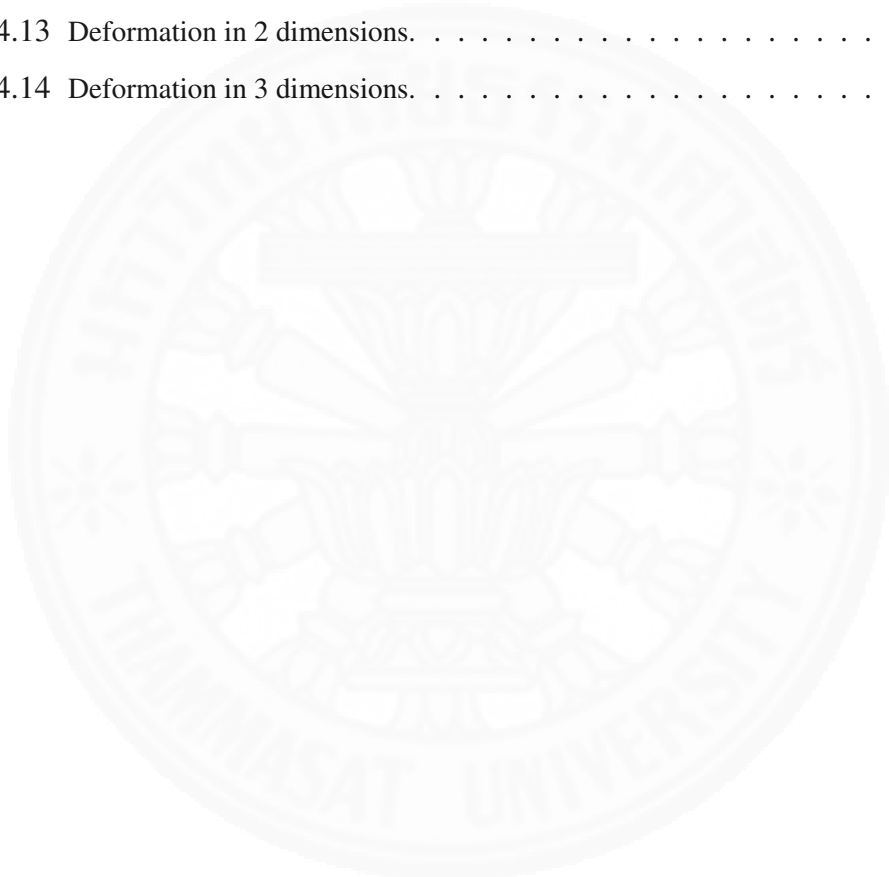
<b>4</b>	<b>THE COMBUSTION OF BIO-COAL PELLETS WITH BOUNDARY MOVEMENT</b>	<b>43</b>
4.1	General Overview . . . . .	43
4.2	Model Formulation . . . . .	44
4.2.1	Heat Transfer . . . . .	46
4.2.2	Mass Transfer . . . . .	47
4.2.3	Moving Mesh (ALE) . . . . .	49
4.2.4	Initial and Boundary Conditions . . . . .	50
4.3	Method of Solution . . . . .	54
4.4	Results and Discussion . . . . .	56
4.5	Conclusion . . . . .	62
<b>5</b>	<b>SUMMARY AND CONCLUSIONS</b>	<b>63</b>

## LIST OF FIGURES

1.1	The general of the bio-coal production process . . . . .	3
3.1	Bio-coal pellet geometry. . . . .	30
3.2	Boundary setting of heat transfer on the studied bio-coal pellet. . . . .	31
3.3	Boundary setting of mass transfer on bio-coal pellet. . . . .	32
3.4	Finite element mesh of 8482 Lagrange order one tetrahedral element with 1738 nodes . . . . .	34
3.5	Arrow and surface plots of heat transfer of the bio-coal pellet . . . . .	35
3.6	Arrow and surface plots of mass transfer of the bio-coal pellet . . . . .	37
3.7	Slice plots of heat transfer ( $a_1$ ) – ( $a_3$ ) and mass transfer ( $b_1$ ) – ( $b_3$ ) when $C_p = 1380 J/(kg \cdot K)$ at $t=30s, 120s,$ and $240s$ . . . . .	38
3.8	Slice plots of heat transfer ( $a_1$ ) – ( $a_3$ ) and mass transfer ( $b_1$ ) – ( $b_3$ ) when $C_p = 1726 J/(kg \cdot K)$ at $t=30s, 120s,$ and $240s$ . . . . .	39
3.9	Slice plots of heat transfer ( $a_1$ ) – ( $a_3$ ) and mass transfer ( $b_1$ ) – ( $b_3$ ) when $k = 0.311 W/(m \cdot K)$ at $t=30s, 120s,$ and $240s$ . . . . .	40
3.10	Slice plots of heat transfer ( $a_1$ ) – ( $a_3$ ) and mass transfer ( $b_1$ ) – ( $b_3$ ) when $k = 0.185 W/(m \cdot K)$ at $t=30s, 120s$ and $240s$ . . . . .	41
4.1	The sides of bio-coal pellet in 3 dimensions . . . . .	45
4.2	The size of bio-coal pellet in 2 and 3 dimensions . . . . .	46
4.3	The boundary condition of heat transfer model of bio-coal pellet. . . . .	51
4.4	The boundary condition of mass transfer model of bio-coal pellet. . . . .	51
4.5	The boundary condition of mass transfer model of gas. . . . .	52
4.6	Finite element mesh of 374 Lagrange order one tetrahedral element with 209 nodes in 2 dimensions. . . . .	55



4.7	Finite element mesh of 6445 Lagrange order one tetrahedral element with 1588 nodes in 3 dimensions. . . . .	56
4.8	The arrow plot of heat transfer in 2 dimensions. . . . .	57
4.9	The arrow plot of heat transfer in 3 dimensions. . . . .	57
4.10	The heat transfer in 2 dimensions at time=30s, 100s and 180s. . . . .	58
4.11	The heat transfer in 3 dimensions at time=30s, 100s and 180s. . . . .	59
4.12	The heat transfer at t=2.5s and 6.8s. . . . .	60
4.13	Deformation in 2 dimensions. . . . .	61
4.14	Deformation in 3 dimensions. . . . .	61



# **CHAPTER 1**

## **INTRODUCTION**

The world population has increased to over 7 billion in the 21st century and continues to increase. The ever increasing population increases energy demand. However, the energy from fossil fuels is limited. In Thailand, energy security is one of the most important policies, since energy is a basic factor in the people's livelihood. It is also an important factor of production in the business and industrial sectors. When global energy demand continues to rise, especially in the industrial sector, energy security concerns become ever more important. The awareness of renewable energy technologies is increasing, and thermochemical conversion of biomass is one of the most promising non-nuclear forms of future energy. Biomass is a widely utilized source of energy. It is low cost and indigenous in nature. It accounts for almost 15 percent of the world's energy supply and as much as 35 percent in developing countries, used mostly for cooking and heating. If governments desire to use biomass as an alternative energy, they have to find a range of raw materials, and to develop production technologies with the highest efficiency.

Biomass is a biological material derived from animals and plants. Many of the biomass fuels used today come in the form of wood products, crop residues, dried vegetation and aquatic plants. Some kinds of biomass can be burned to produce energy; the most common example being wood. Biomass contains stored energy because plants capture energy from the sun through the process of photosynthesis, so when biomass is burned, this stored energy is released as heat. When biomass is burned, it releases carbon dioxide but plants also take this gas out of the atmosphere throughout their lifetime for using it to grow.

Among the variation in chemical composition of biomass are several factors such as low energy density, high moisture content and high oxygen content that affect any process.

When using untreated biomass, the nature of biomass is relevant. For instant, if biomass is directly used for energy production, much higher load of biomass is required to produce the same amount of energy as fossil fuels [20]. Most of the energy obtained from biomass serves to remove moisture, so a lower moisture content leads to the release of more energy.

Over the last 20 years, there have been many efforts to study and improve the quality of biomass. Biomass materials are extremely complex and there are many steps needed to produce the biomass. Torrefaction is a process used to produce high-grade solid bio-fuels from various streams of woody biomass. It is a thermal process of biomass that is also referred to as slow pyrolysis, at temperatures typically between 200 °C and 320 °C, in an inert atmosphere. Torrefaction changes the biomass properties to provide a better fuel for combustion and gasification. During the torrefaction, the biomass dries completely and turns into solid products and volatiles which the volatiles include condensable liquids and non-condensable gases. The final product is the remaining solid, dry and blackened material, technically known as “torrefied wood or bio-coal”. Moreover, biomass is forced to decompose into liquids and gases. To development of highly efficient torrefaction of biomass, in combination with densification (pelletisation or briquetting), is a promising step in overcoming logistic challenges in large-scale biomass production, it is easier to transport and store.

The general process of making bio-coal entails three different phases: the pre-drying phase of the biomass, the pyrolysis or torrefaction phase, and the cooling phase of treated biomass. The thermal treatment process depending on the peak temperature, bio-coal is first cooled, after that it can be pelletised or briquetted for transportation or storage. Bio-coal can be directed toward combustion if it is intended for energy production. In the production of bio-coal, volatile gases and liquids are normally separated from the system, such liquids and gases products can be used for combustion into transportation fuels. The general of the process appears in Figure 1.1 [20].

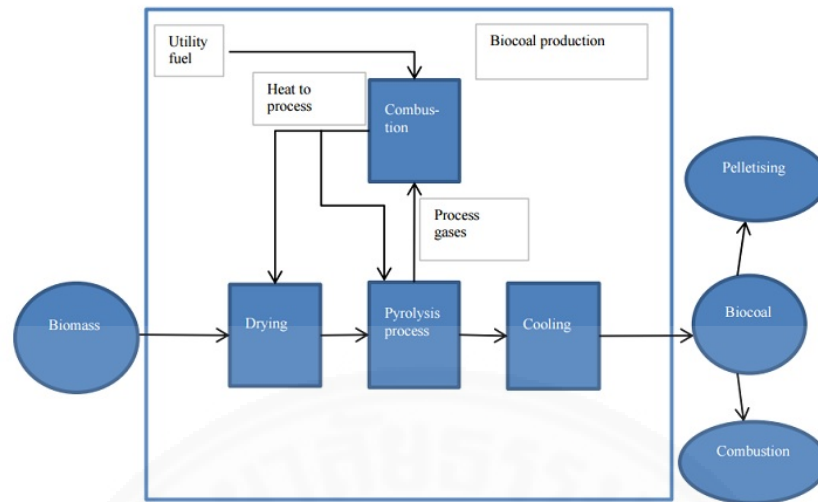


Figure 1.1: The general of the bio-coal production process

Since the quality of biomass depends on many properties, such as physical characteristics, heating value, high bulk density, and moisture content, its study is rather complex. There are many ways to study the potential of biomass, such as direct experiments, theoretical analysis, and mathematical models. Mathematical models and theoretical analysis can explain phenomena of biomass more cheaply than experimental approaches. Mathematical modeling is an effective tool in the implementation of appropriate management.

However, the biomass used for fuel, especially for electricity production, presents challenges in materials handling and combustion efficiency.

### 1.1 Heat and Mass Transfer

The heat transfer describes the exchange of thermal energy between physical system which depend on the temperature. Heat transfers from a region of higher temperature to another region of lower temperature. The three fundamental modes of heat transfer are conduction, convection, and radiation. Mass transfer describes the transport of mass from one location to another and takes place in a single phase or over phase boundaries in multiphase system. The mass transfer occurs in many processess such as evaporation, absorption, adsorption, and drying. In majority of engineering problems, mass

transfer involves at least gas or liquid phase and may also be described in solid phase materials. The phase is used in engineering for physical process that involves diffusive and convective of chemical species. The mass transfer of species takes place together with chemical reactions which can be implied that flux of a chemical species does not have to be conserved in a volume element since chemical species may be produced or consumed in such an element [4]. Mass transfer theory allows for the computation of mass flux in a system and mass distribution of different species overtime and space [4].

## 1.2 The Combustion Process

Combustion is a chemically reaction of a fuel combine with oxygen in the air to release heat which similar to photosynthesis in reverse. This process is used in households every day for heating and cooking and in industries for generating heat or steam [19].

For combustion, good fuels are materials rich in hydrogen and carbon. All hydrogen and carbon are split off and combined with the oxygen in the air to create carbon dioxide, heat, and water vapor. The main products in burning biomass are water and carbon dioxide.

The combustion has three requirements; heat, fuel, and air. There must be fuel to burn, air to supply oxygen and heat to start and continue the combustion process. When the three requirement are available, combustion is self-sustaining because the fuel release excess heat to initiate further burning and if any of these three are removed, burning stops [19].

For the solid biomass to be converted into useful heat energy, there are three main stages to the combustion process.

**Heating and Drying:** The moisture in biomass has to be driven off before combustion can takes place. The heat for drying is supplied by radiation from flames and from stored heat in side the body of the combustion unit [19].

**Pyrolysis:** When the temperature is raised between 200 °C and 350 °C, the volatile gases are released. The products in this stage include carbon dioxide, carbon monoxide and methane which these gases mix with oxygen from the air and burn producing a

yellow flame. After the volatiles have been burned off, char is the remaining material.

**Oxidation:** The char oxidizes or burns where oxygen is required again. Long residence time for fuel in the combustor allows the fuel to be completely consumed.

It is important to attempt for complete combustion to improve the cost efficiency and preserve fuel in the combustion process. In the combustion chamber, there must be enough air for complete combustion to occur.

Although, the mathematical modeling of heat transfer of biomass has been undertaken for decades, there have been little mathematical modeling of heat transfer in the combustion of bio-coal. It is necessary to develop a more robust mathematical model and numerical simulations for heat transfer in bio-coal combustion.

### 1.3 Scope and Objectives of the Research

Even though, the study of the complex phenomena in the combustion of biomass has been carried out for many years, least number of research present a mathematical model to simulate heat transfer on bio-coal pellets in the combustion process. There are several works studied about mathematical modelling of heat and mass transfer in the process of biomass, but now there is no the best model and no attempt has been coupled heat and mass transfer to the moving boundary of the bio-coal pellet in the combustion process. In addition, torrefaction process is a new technology that increase efficiency of biomass in being on fire and pelletization to bio-coal pellets. The bio-coal is more convenient to use in the next process and it is a new evolution of biomass. Moreover, the study which simulate heat and mass transfer couple with boundary moving by using COMSOL Multiphysic for bio-coal pellets is never presented. For this reason, we are so interested to present mathematical models that can simulate heat and mass transfer occuring in the process of combustion on bio-coal.

In this research, we study the combustion of bio-coal pellets in cylindrical shape which start burning at one side. We consider the heat and mass transfer in transient state problem. Since the potential of the now a days computer can be made easily and quickly to understand the phenomenon. Thus, to get the new ideas of the research, the objectives are as follows.

1) to develop a mathematical model to explain heat and mass transfer on a bio-coal pellet when it is burned in the combustion process,

2) to investigate the influence of the parameters thermal conductivity and heat capacity on the heat and mass transfer,

3) to develop a coupled heat and mass transfer and moving boundary model to describe the contraction behavior of a bio-coal pellet when it is burned in the combustion process.

Both presented models are solved by using finite element method in COMSOL Multiphysics software.

#### **1.4 Outline of the Thesis**

This thesis consists of five chapters. Chapter One presents the introduction of this research. The phenomena, properties and quality of biomass, are described in the first section. The scope and objectives of this research in the second section. The outline of the thesis is given in the third section.

Chapter Two concerns the literature reviews of previous works which related to our study. Previous studies of heat and mass transfer models in the process of biomass is reviewed in Section 2.1. Related works on free surface and boundary movement in COMSOL Multiphysics are given in Section 2.2.

Chapter Three presents the mathematical model of the numerical simulation of the study heat and mass transfer by using an algorithm based on the finite element method. The governing equations, the initial and boundary conditions are presented in Section 3.2. The finite element method to solve the problem is given in Section 3.3. The results of the numerical investigation and the effect of the materials on heat and mass transfer are presented in Section 3.4.

Chapter Four presents the mathematical model of the heat and mass transfer models coupled with free surface movement and numerical simulation of the model by using of the Arbitrary Lagrangian-Eulerian technique. The mesh velocity is introduced in the rate of mass reduction or the rate of gas growth form.

Chapter Five presents the conclusions gained from the research.

## CHAPTER 2

### LITERATURE REVIEWS

There have been many studies of biomass pellets. Initially research, we focus on the mathematical modeling of all biomass products, in particular, we focus on the research that improves the quality of biomass pellet burning and the use of biomass, such as pyrolysis, gasification and the torrefaction.

#### 2.1 Heat and Mass Transfer

In 1998, Jalan and Srivastava [12] developed a mathematical model to describe the pyrolysis of a single solid biomass particle, including the phenomena of biomass based on physical and chemical changes. The chemical changes include primary and secondary pyrolysis reactions, controlled by the heat transfer phenomena. The used numerical schemes was a finite difference, backward implicit scheme for the heat transfer equation and the 4th Order Runge-Kutta Predictor Corrector method for the chemical kinetics equation. The model of Kung considered heat transfer caused conduction, internal heat convection of volatiles and first order kinetics for formulation of volatiles and char.

In this approach a biomass particle is heated in an inert atmosphere. First step, heat is transferred to the particle surface by radiation or natural convection, then transferred to the inside of the particle by conduction. Therefore, the temperature inside increases, removing the moisture in the biomass particle. The effect of heat transfer results in a phase change and this contributes to a temperature gradient as a function of time, which is nonlinear [12]. Gaseous products including volatiles are involved in the transfer of heat, and the change of density.



For simplicity, it is assumed that heat inside the solid particle is transferred by conduction, and the effect of porosity is not considered for this work. As the temperature inside the particle increases over time, greater quantities of volatiles and gases are formed. Changes in heating conditions alter the reaction rate and affect the overall pyrolysis rates.

Jalan and Srivastava[12] considered a cylindrical shell of radius  $r$  and length  $z$ . They founded that heat transfer occurs only the radial direction and takes place within the particle by conduction only.

The generalized form of the heat equation is developed as follows:

$$k \left[ \frac{1}{r} \frac{dT}{dr} + \frac{d^2T}{dr^2} \right] + (-\Delta H) \frac{d(-\rho)}{dt} = \frac{d(\rho C_P T)}{dt} \quad (2.1)$$

where  $C_P$  is specific heat ( $J/(kg \cdot K)$ ), which is considered to be independent of time. Since,  $C_P$  is a function of temperature when temperature is a function of time, so, the  $C_P$  value is taken as a function of temperature:

$$k \left[ \frac{1}{r} \frac{dT}{dr} + \frac{d^2T}{dr^2} \right] + (-\Delta H) + C_P T \frac{d(-\rho)}{dt} = \rho C_P \frac{dT}{dt}, \quad (2.2)$$

where  $k$  is thermal conductivity ( $W/m \cdot K$ ),  $r$  is radial distance ( $m$ ),  $\delta H$  is heat of reaction ( $kJ/kg$ ),  $T$  is temperature ( $K$ ),  $\rho$  is density ( $kg/m^3$ ), and  $t$  is time ( $s$ ).

The variation of  $C_p$  and  $k$  is based on the equation as given by

$$C_P = 1112 + 4.85(T - 273), \quad (2.3)$$

$$k = 0.13 + 0.0003(T - 273). \quad (2.4)$$

The initial condition is set as

$$t = 0, T(r, 0) = T_0, \quad (2.5)$$

and the boundary conditions are

$$t > 0, r = 0, \frac{dT}{dr} = 0, \quad (2.6)$$

$$t = 0, r = R, \left( -k \left( \frac{dT}{dr} \right) \right) = h(T_f - T) + \sigma \epsilon (T_f^4 - T^4). \quad (2.7)$$

Where  $h$  is convective heat transfer coefficient ( $W/m^2 \cdot K$ ),  $T_f$  is final temperature ( $K$ ),  $\sigma$  is Stefan Boltzman constant,  $\epsilon$  is emissivity coefficient.

The results of the paper present the effect of particle size on the temperature profile as a function of the radial distance at varying time intervals. The results from the model are compared with experimental data from the literature.

In 2003, Babu and Chaurasia [1] used a mathematical model to describe the pyrolysis of a single solid particle of biomass, coupling the heat transfer with the chemical kinetics equations. The assumption is that the convective heat transfer coefficient depends on the Reynolds number and the Prandtl number. For solving the heat transfer equation, an implicit scheme of the finite difference method and the Runge-Kutta 4th order method for the chemical kinetics equation are used. The model is solved for cylindrical pellets, slab geometries and spheres on radius ranging from 0.00025 to 0.013 m and temperatures ranging from 303 to 1000 K.

The used kinetic equation are as follows:

$$\frac{dC_B}{dt} = -k_1 C_B^{m_1} - k_2 C_B^{m_1}, \quad (2.8)$$

$$\frac{dC_{G_1}}{dt} = k_1 C_B^{m_1} - k_3 C_{G_1}^{m_2} C_{C_1}^{m_3}, \quad (2.9)$$

$$\frac{dC_{C_1}}{dt} = k_2 C_B^{m_1} - k_3 C_{G_1}^{m_2} C_{C_1}^{m_3}, \quad (2.10)$$

$$\frac{dC_{G_2}}{dt} = k_3 C_{G_1}^{m_2} C_{C_1}^{m_3}, \quad (2.11)$$

$$\frac{dC_{C_2}}{dt} = k_3 C_{G_1}^{m_2} C_{C_1}^{m_3}, \quad (2.12)$$

where

$$k_1 = A_1 \exp[(D_1/T) + (L_1/T^2)],$$

$$k_2 = A_2 \exp[(D_2/T) + (L_2/T^2)],$$

$$k_3 = A_3 \exp[(-E_3/R_c T)].$$

Where  $C_B$  is concentration of virgin biomass ( $kg/m^3$ ),  $C_{G_1}$  is concentration of gases and volatiles 1 ( $kg/m^3$ ),  $C_{C_1}$  is concentration of char 1 ( $kg/m^3$ ),  $C_{G_2}$  is concentration of gases and volatiles 2 ( $kg/m^3$ ),  $C_{C_2}$  is concentration of gases and volatiles 2 ( $kg/m^3$ ),  $n_1, n_2, n_3$  are orders of reaction, dimensionless,  $k_1, k_2, k_3$  are rate constants ( $s^{-1}$ ),  $R_c$  is universal gas constant ( $J/mol$ ).

After the combining of Eq. (2.8), (2.10) and (2.12), the result is

$$\frac{dC_B}{dt} + \frac{dC_{C_1}}{dt} + \frac{dC_{C_2}}{dt} = -k_1 C_B^{n_1}, \quad (2.13)$$

which is equal to  $d\rho/dt$ . Hence,

$$\frac{d\rho}{dt} = -k_1 C_B^{n_1}. \quad (2.14)$$

The heat transfer equation is given by

$$(C_P)\rho \frac{dT}{dt} = k \left( \frac{b-1}{r} \frac{dT}{dr} + \frac{d^2T}{dr^2} \right) + [(-\Delta H) + C_P T] \left( \frac{d(-\rho)}{dt} \right). \quad (2.15)$$

The initial and boundary conditions are set as:

$$t = 0, T(r, 0) = T_0, \quad (2.16)$$

$$t > 0, r = 0, \left( \frac{dT}{dr} \right)_{r=0} = 0, \quad (2.17)$$

$$t > 0, r = R, -k \left( \frac{dT}{dr} \right)_{r=R} = h(T_f - T) + \sigma \epsilon (T_f^4 - T^4). \quad (2.18)$$

Where  $\rho$  is density ( $kg/m^3$ ),  $k$  is thermal conductivity ( $W/m \cdot K$ ),  $r$  is radial distance ( $m$ ),  $\Delta H$  is heat of reaction ( $J/kg$ ),  $C_P$  is specific heat ( $J/kg \cdot K$ ),  $b$  is geometry factor,  $T$  temperature  $K$ ,  $\sigma$  is Stefan Boltzman constant ( $W/m^2 \cdot K^4$ ),  $\epsilon$  is emissivity coefficient,  $T_f$  is final temperature  $K$ ,  $h$  is convective heat transfer coefficient ( $W/m^2 \cdot K$ ).

The results show the temperature profile as a function of radial distance at the time of completion. They observed that the dimensions of the particle increase and the time required for completion also increases. The temperature profiles as a function of radial

distance are also shown at various times. It is observed that as the time of pyrolysis increases, the temperature increases. This can be explained by heat transfer due to radiation and convection from the wall surface. The resistance offered for heat transfer near the wall is very high.

Then, in 2004, Babu and Chaurasia [2] proposed a generalized model incorporating chemical processes, including heat conduction, convection and radiation, transport of volatiles and gas by diffusion and convection, and momentum transfer. A finite difference implicit scheme utilizing a Tri-Diagonal Matrix Algorithm is used for solving the heat and mass transfer equations and a Runge-Kutta 4th order method for the chemical kinetics equations. The simulations are present for radii ranging from 0.0001 to 0.017 m and temperatures ranging from 303 to 2800 K. The improved model is utilized to investigate the influence of particle size and shape, product distribution, conversion heat and time of reaction. The results show the effect of temperature on particle size and on conversion time of pyrolysis, the effect of particle size and shape on conversion time and on product yield and the effect of the heat of reaction number on biomass conversion, temperature and biomass concentration.

Mass conservation is given by

$$\frac{\partial C_B}{\partial t} = -k_1 C_B^{m_1} - k_2 C_B^{m_1}, \quad (2.19)$$

$$\frac{\partial(C_{G_1} \varepsilon'')}{\partial t} + \frac{\partial(C_{G_1} u)}{\partial r} = D_{eG_1} \left( \frac{b-1}{r} \frac{\partial C_{G_1}}{\partial r} + \frac{\partial^2 C_{G_1}}{\partial r^2} \right) + k_1 C_B^{m_1} - \varepsilon'' k_3 C_{G_1}^{m_2} C_{C_1}^{m_3}, \quad (2.20)$$

$$\frac{\partial C_{C_1}}{\partial t} = k_2 C_B^{m_1} - k_3 C_{G_1}^{m_2} C_{C_1}^{m_3}, \quad (2.21)$$

$$\frac{\partial C_{G_2}}{\partial t} = k_3 C_{G_1}^{m_2} C_{C_1}^{m_3}, \quad (2.22)$$

$$\frac{\partial C_{C_2}}{\partial t} = k_3 C_{G_1}^{m_2} C_{C_1}^{m_3}. \quad (2.23)$$

Where  $C_B$  is concentration of virgin biomass ( $kg/m^3$ ),  $C_{G_1}$  is concentration of gases and volatiles 1 ( $kg/m^3$ ),  $C_{C_1}$  is concentration of char 1 ( $kg/m^3$ ),  $C_{G_2}$  is concentration of gases and volatiles 2 ( $kg/m^3$ ),  $C_{C_2}$  is concentration of gases and volatiles 2

( $kg/m^3$ ),  $n_1, n_2, n_3$  are orders of reaction, dimensionless,  $k_1, k_2, k_3$  are rate constants ( $s^{-1}$ ),  $D_{eG_1}$  is effective diffusivity of gas and volatiles 1 ( $m^2/s$ ),  $u$  is gas velocity ( $m/s$ ),  $\varepsilon''$  is void fraction of particle,  $b$  is geometry factor, and  $r$  is radial distance ( $m$ ).

Enthalpy is given by

$$\frac{\partial}{\partial t}(C_p \rho T) = k \left( \frac{b-1}{r} \frac{\partial T}{\partial r} + \frac{\partial^2 T}{\partial r^2} \right) - \left( D_{eG_1} \frac{\partial C_{G_1}}{\partial r} \right) C_{pG_1} \frac{\partial T}{\partial r} + (-\Delta H) \left( -\frac{\partial \rho}{\partial t} \right). \quad (2.24)$$

Where  $\rho$  is density ( $kg/m^3$ ),  $k$  is thermal conductivity ( $W/mK$ ),  $\delta H$  is heat of reaction ( $J/kg$ ),  $C_P$  is specific heat ( $J/mol \cdot K$ ),  $T$  temperature  $K$ ,  $C_{pG_1}$  is heat capacity of gases and volatiles 1 ( $J/mol \cdot K$ ).

The results can be explained as follows. The average particle temperature at various radial point increase when the particle radius is increased. This results are different for different shapes as same as the result of different heat penetration. As the particle radius increases, the time for completion of pyrolysis also increases. As the final furnace temperature is increased to 2100 K, the concentration of biomass decreases up to a time of 74 s. The biomass conversion is more sensitive to the heat of reaction number when it is negative rather than positive. The results show that the temperature increases with radial distance for different values of time. For the effect of the heat of reaction number on the biomass concentration, it is seen that the concentration increases at the center and decreases at the surface as pyrolysis progresses.

In 2005, Porteiro et al.[16] studied a mathematical model of the combustion of a single wood particle and described the thermal degradation of biomass. The model uses a novel discretisation scheme and combines intra-particle combustion with extra-particle transport, including thermal and diffusional mechanisms. During degradation, the influence of structural changes of the wood in different stages is studied together with particle shrinkage. The study considers a generalized cylindrical particle with initial radius  $R$  and length  $L$ . The scheme is based on the assumption that if the particle and the external conditions are isotropic, every point at a determined distance from the surface will show the same state of degradation.

To formulate the model, heat transfer, diffusive and convective mass transport inside the particle and the transient diffusive chemical reactions around the particle are

described by setting the conservation equations to appropriate initial and boundary conditions. The conservation is described by the general differential equation:

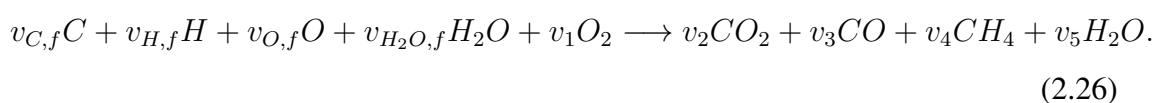
$$\frac{\partial}{\partial t}(\psi_i, \varphi_i) + \frac{1}{G(r)} \frac{\partial}{\partial r}(G(r)\psi_i u \varphi_i) = \frac{1}{G(r)} \frac{\partial}{\partial r}(G(r)\Gamma_i \frac{\partial \varphi_i}{\partial r}) + S_i. \quad (2.25)$$

Where  $\psi_i$  is the generalized densities,  $\varphi_i$  is the dependent variable,  $G(r)$  is the area of the control surface at a predetermined position  $r$  ( $m^2$ ),  $r$  is the radial coordinate ( $m$ ),  $u$  is gas velocity ( $m/s$ ),  $\Gamma_i$  is the diffusion coefficient, and  $S_i$  is the source/sink term.

The main reactions during heterogeneous combustion include water vaporization, devolatilization and combustion/gasification of char. The heterogeneous reaction of char with the gas phase is assumed to be limited, and then gas phase is oxidize to produces carbon dioxide and carbon monoxide. The obtain results show that under combustion, the char reaction is normally controlled by the diffusion of oxygen from bulk. Under diffusional control conditions, a char reaction occurs on the surface of the particle. Hence, the particle shrinks during the heterogeneous phase of combustion.

As predicted by the model, when the inside particle reaches its drying temperature, particle drying is almost complete and 20 percent of the mass has already been lost. The drying rate starts with a peak and then drops until completion, while the highest reaction rate for pyrolysis is reached later when the absence of moisture in the external layers allows them to heat up. The char oxidation rate becomes transport controlled when the temperature of the outer layer is high enough. Therefore, char consumption becomes a surface phenomenon and causes the particle to shrink.

In 2007, Ferrero et al.[8] developed a numerical model for predicting the possibility of occurrence of self-ignition in stored biomass, coal heaps, and dump deposits. Self-ignition is caused by low-rate exothermic reaction and low-temperature within the deposit of material. The combustion process can be described by general equation as follows:



Chemical species include fuel, oxygen, carbon monoxide, carbon dioxide, methane, and water.

The temperature and concentration are solved with Fourier-type and Fick-type equations, respectively:

$$\frac{\partial T}{\partial t} = \frac{\lambda}{\rho \cdot c_P} \cdot \nabla \cdot (\nabla T) + S_T, \quad (2.27)$$

$$\frac{\partial C_k}{\partial t} = D_k \cdot \nabla \cdot (\nabla C_k) + S_{C_k}. \quad (2.28)$$

Where  $T$  is the temperature ( $K$ ),  $t$  is time ( $s$ ),  $\lambda$  is the thermal conductivity ( $W/m \cdot K$ ),  $\rho$  is the bulk density ( $kg/m^3$ ),  $c_P$  is the specific heat ( $J/kg \cdot K$ ),  $S_T$  is the heat production term ( $W/m^3$ ),  $C_k$  is the mass concentration of the species  $k$  ( $kg/m^3$ ),  $D_k$  is the diffusion coefficient of the species  $k$  ( $m^2/s$ ), and  $S_{C_k}$  is the production rate of the species  $k$  ( $W/m^3$ ).

For the decomposition of the solid fuel, an Arrhenius reaction rate are given as follows:

$$\frac{\partial C_f}{\partial t} = -C_f \cdot k_0 \cdot \exp\left(-\frac{E}{RT}\right). \quad (2.29)$$

Where  $C_f$  is the mass concentration of fuel ( $kg/m^3$ ),  $k_0$  is the pre-exponential factor ( $1/s$ ),  $E$  is the activation energy ( $J/mol$ ), and  $R$  is the universal gas constant ( $J/mol$ ).

For solving the system of equations in this case, the commercial Finite Element Code COMSOL Multiphysics is used which can be describe generation and propagation of fires in large scale deposits of combustible bulk materials. The result shown the comparison of numerically simulated and experimentally determines self-ignition temperatures of the investigated woods which are in good agreement.

In 2008, Yao et al.[21] studied the combustion of a single particle of biomass. The behavior of a single biomass is fundamental to all practical applications, including fluidized-bed and pack-bed combustion, as well as pulverized fuel suspended combustion. The considered single biomass particle range in size from  $10\mu m$  to  $20mm$ . The sensitivity to the variation in parameters, especially the particle size and heating rates are investigated. In addition, this work examines the different sub-proceses such as moisture evaporation, devolatilization, char combustion, tar cracking, and gas-phase reactions. The results of the study are useful for assessing systems of diferrent combustion that use biomass as a fuel. The results also help to clarify situations in which the thermally thin and thick cases interface.

This paper studied a cylindrical particle of biomass in two-dimensions, surrounded by a passing gas stream. Under conditions of combustion, the temperature gradient inside a particle is much higher, the burning process, and the ash layer formed are never one-dimensional in terms of the particle radius. Experiments on small single particles using thermogravimetric analysis (TGA), entrained particle combustion in a supporting flame, and suspended combustion were conducted. In experimental study, they use TGA with small particles of low heating rate and mass, where can be severe consequences for the kinetic data arising from secondary reactions, especially in the larger particles.

Yao's used the FLUENT code to gave the history of temperature devolatilisation, but also used the assumption of uniform particle temperature. The result shows that the effects of particle size and temperature are very marked and the particle size are dictate the temperature and devolatilisation rates. In order to study the larger particle sizes (5 – 35mm), a stationary packed-bed reactor is used which is a vertical cylindrical combustion chamber with diameter 200 mm. The mass loss rate of this reaction is determined gravimetrically and the histories of mass loss for different sizes make it clear that the larger particles react more slowly.

In this paper, many process and model are examined and described such as:

**Heat and mass transfer.** The model studies on the cylindrical coordinates of a small particle inside the computation domain. The exchange of energy and mass species occurs through the boundary layer and the exchange of radiation heat between the particle external surface and the surrounding environment. The main gas flow passing around the particle and the properties of the inlet main flow include temperature, uniform velocity, and species concentrations such as  $O_2$ ,  $N_2$  and  $CO_2$ . The solid species include volatile, moisture, fixed carbon and ash inside the particle. The components are immobilized, while Fick's law is valid for gaseous species transport.

This paper describes the transport equation of the gas phase as follows:

Continuity:

$$\frac{\partial(\phi\rho_g)}{\partial t} + \frac{\partial(\phi\rho_g u_x)}{\partial x} + \frac{\partial(r\phi\rho_g u_r)}{r\partial r} = r_M + r_V + r_C, \quad (2.30)$$



$x$ -momentum:

$$\begin{aligned} \frac{\partial(\phi\rho_g u_x)}{\partial t} + \frac{\partial(\phi\rho_g u_x u_x)}{\partial x} + \frac{\partial(r\phi\rho_g u_r u_x)}{r\partial r} = -\frac{\phi p_g}{\partial x} - \frac{\mu}{K} u_x \\ + 2\frac{\partial}{\partial x} \left( \mu \frac{\partial u_x}{\partial x} \right) + \frac{\partial}{r\partial r} \left( r\mu \left( \frac{\partial u_x}{\partial r} + \frac{\partial u_r}{\partial x} \right) \right), \end{aligned} \quad (2.31)$$

$y$ -momentum:

$$\begin{aligned} \frac{\partial(\phi\rho_g u_r)}{\partial t} + \frac{\partial(\phi\rho_g u_x u_r)}{\partial x} + \frac{\partial(r\phi\rho_g u_r u_r)}{r\partial r} = -\frac{\phi p_g}{\partial r} - \frac{\mu}{K} u_r \\ + 2\frac{\partial}{r\partial r} \left( r\mu \left( \frac{\partial u_r}{\partial r} \right) \right) + \frac{\partial}{\partial x} \left( \mu \left( \frac{\partial u_x}{\partial r} + \frac{\partial u_r}{\partial x} \right) \right) - 2\mu \frac{u_r}{r^2}, \end{aligned} \quad (2.32)$$

Gaseous species:

$$\begin{aligned} \frac{\partial(\phi\rho_g Y_i)}{\partial t} + \frac{\partial(\phi\rho_g u_x Y_i)}{\partial x} + \frac{\partial(r\phi\rho_g u_r Y_i)}{r\partial r} = \frac{\partial}{\partial x} \left( D_g^* \frac{\partial(\phi\rho_g Y_i)}{\partial x} \right) \\ \frac{\partial}{r\partial r} \left( rD_g^* \frac{\partial(\phi\rho_g Y_i)}{\partial r} \right) + \sum_{j=1}^{j=N} r_{ij}. \end{aligned} \quad (2.33)$$

Where  $\phi$  is the porosity inside a particle,  $\rho_g$  is the density of gas ( $kg/m^3$ ),  $t$  is time ( $s$ )  $u_x$  is the velocity in axial direction ( $m/s$ ),  $u_r$  is the velocity in axial direction ( $m/s$ ),  $x$  is radial coordinate ( $m$ ),  $r$  is radial coordinate ( $m$ ),  $u_r$  is the velocity in radial direction ( $m/s$ ),  $r_M$  is the process rate of moisture evaporation ( $kg/m^3 \cdot s$ ),  $r_V$  the process rate of volatile release ( $kg/m^3 \cdot s$ ),  $r_C$  is the process rate of char burnout ( $kg/m^3 \cdot s$ ),  $p_g$  is pressure of gas ( $Pa$ ),  $\mu$  is gas viscosity,  $K$  is permeability ( $m^2$ ),  $Y_i$  is species mass fraction, and  $D$  is diffusion coefficient.

Energy:

$$\begin{aligned} \phi\rho_g \frac{\partial H_g}{\partial t} + \frac{\partial(\phi\rho_g u_x H_g)}{\partial x} + \frac{\partial(r\phi\rho_g u_r H_g)}{r\partial r} = \frac{\partial}{\partial x} \left( k_{eff} \phi\rho_g C_{pg} \frac{\partial T_g}{\partial x} \right) \\ + \frac{\partial}{r\partial r} \left( r k_{eff} \phi\rho_g C_{pg} \frac{\partial T_g}{\partial r} \right) + \sum_{j=1}^{j=N} r_j \Delta H_j + (1 - \phi) h_{sg} S_a (T_s - T_g). \end{aligned} \quad (2.34)$$

Where  $H_g$  is the enthalpy of gas phase ( $J/kg$ ),  $k_{eff}$  is the effective thermal heat transfer coefficient,  $T_g$  is the temperature of gas phase ( $K$ ),  $T_s$  is the temperature of solid phase ( $K$ ),  $h_{sg}$  is the gas-to-solid heat transfer coefficient ( $(W/m^2 K)$ ),  $\Delta H$  is the reaction rate ( $J/kg$ ), and  $S_a$  is the surface area ( $m^2$ ).

The mass loss rate for the solid phase is described by

$$\frac{d((1 - \phi)\rho_s V_p)}{dt} = -V_p (r_M + r_V + r_C). \quad (2.35)$$

Where  $\rho_s$  is the density of solid ( $kg/m^3$ ),  $V_p$  is the particle volume ( $m^3$ ).

Energy conservation,

$$(1 - \phi)\rho_s \frac{\partial H_s}{\partial t} = \frac{\partial}{\partial x} \left( k_{eff}^s \frac{\partial T_s}{\partial x} \right) + \frac{\partial}{r \partial r} \left( k_{eff}^s \frac{\partial T_s}{\partial r} \right) + r \dot{M} \Delta H_M \quad (2.36)$$

$$+ r \dot{V} \Delta H_V + r \dot{C} \Delta H_C + (1 - \phi) h_{sg} S_a (T_g - T_s) + Q_{ext}.$$

Where  $H_s$  is the enthalpy of solid phase ( $J/kg$ ),  $\Delta H_M$  is the reaction rate of moisture evaporation ( $J/kg$ ),  $\Delta H_V$  is the reaction rate of volatile release ( $J/kg$ ),  $\Delta H_C$  is the reaction rate char burnout ( $J/kg$ ), and  $Q_{ext}$  is the external radiation heat transfer to the particle surface.

The relation of the local porosity variation with moisture evaporation, volatile release, and fixed-carbon combustion is given by

$$\phi = \phi_0 + (1 - \phi_0)(\alpha_M(X_{M0} - X_M) + \alpha_V(X_{V0} - X_V) + \alpha_C(X_{C0} - X_C)). \quad (2.37)$$

Where  $\phi_0$  is the initial porosity inside a particle,  $X_M$  is the solid component mass fraction of moisture evaporation,  $X_V$  is the solid component mass fraction of volatile release,  $X_C$  is the solid component mass fraction of char burnout, and the parameters  $\alpha_M$ ,  $\alpha_V$ ,  $\alpha_C$  represent the extent of particle shrinkage during each of the solid-phase processes.

The results of the model are compared between the video images of the burning suspended in a methane flame and the situation depicting the whole combustion from initial heating up to final char burnout with continuous shrinking of the particle and change of shape. The results show that the particle first heats up at the bottom where the boundary layer is the thinnest. As the combustion proceeds, the particle volume shrinks and devolatilisation is also initiated at the top as the local solid temperature exceeds the threshold. The results show the effect of particle size in terms of mass loss. The maximum heating rate is achieved when the released volatiles begin to burn in the gas-phase, so providing extra heat to the particle to accelerate the whole process. It is clear that the heating-up times are significant in a gas flame, high flame temperature and furnace conditions for particle.

In 2009, Prakash and Karunanithi [17] reviewed the various aspects of simulation and modeling in pyrolysis of biomass from 1946 to 2007. They described the vari-

ous modeling approaches adopted, range of parameters achieved, and different kinetic schemes proposed. The dependence on parameters such as temperature, time, size, particle shape and moisture content explain the necessity for further improvement in simulation modeling of this process. The study observes that most models have limiting assumptions and applications to define operating conditions, and the fewest studies are on the composition of single particle models with pyrolysis reactor models.

In 2012, Peng et al.[15] studied the particle size effect on torrefaction of pine and formation of torrefied pellets in a thermogravimetric analyzer (TGA) and tubular fixed bed reactor. The internal diffusion inside the particle imposes an impact on the global torrefaction reaction rate. The hard core or nonshrinkage particle model can predict the reaction data, with the data fitted effective vapor diffusion coefficient. Wood torrefaction is a thermal treatment without oxygen or air in the temperature range 473-573 K. Most previous studies were conducted in fixed bed reactors and developed kinetic models for the torrefaction of softwoods to establish a relationship between weight loss, reaction temperature, and residence time. The effect of these on torrefaction and densification of different wood species were reported. Particle size is an important design parameter for torrefaction and densification, which was not reported in earlier studies.

The results show that the torrefaction rate is affected by the particle size, especially at high temperature. During torrefaction, the particle size affects the weight loss so that when the particle size increases, the weight loss rate decreases. At higher temperatures, the smaller particles lost weight faster than larger ones. Biot and pyrolysis numbers show that the temperature gradient within the particle is very small during torrefaction. The heat is transferred across the boundary layer to the surface and then to the interior by thermal conduction. This implies that heat and mass transfer could influence the torrefaction rate of a large particle.

The heat and mass balance equation are given as

$$\frac{\partial}{\partial t} \rho C_P T = \lambda \left[ \frac{1}{r^2} \frac{\partial}{\partial r} \left( r^2 \frac{\partial T}{\partial r} \right) \right] + \Delta H r_{Reaction}, \quad (2.38)$$

$$\frac{\partial C}{\partial t} = D_m \left[ \frac{1}{r^2} \frac{\partial}{\partial r} \left( r^2 \frac{\partial C}{\partial r} \right) \right] + r_{Reaction}. \quad (2.39)$$

Where  $\rho$  is the density of biomass ( $kg/m^3$ ),  $t$  is the time ( $s$ ),  $C_P$  is the heat capacity

of biomass ( $J/kg \cdot K$ ),  $T$  is the temperature ( $K$ ),  $\lambda$  is the thermal conductivity of biomass ( $W/m \cdot K$ ),  $r_{reaction}$  is the true global reaction rate,  $\Delta_H$  is the decomposition heat of biomass ( $J/m^3$ ),  $C$  is the concentration of volatiles inside particle,  $r$  is the radii of sphere ( $m$ ), and  $D_m$  is the diffusivity of volatiles ( $m^2/s$ )

The concentration inside the particle over time reduces to

$$D_m \left[ \frac{1}{r^2} \frac{d}{dr} r^2 \frac{dC}{dr} \right] + k_r C = 0, \quad (2.40)$$

the boundary conditions are

$$\left. \frac{dC}{dr} \right|_{r=0} = 0, C|_{r=R} = C_R. \quad (2.41)$$

Where  $k_r$  is the real intrinsic reaction constant ( $1/s$ ) and  $C_R$  is the concentration of volatiles in particle surface.

Deep torrefaction reduces the pellet expansion, and the quality of pellets from small particles seems to be better than from large particles.

In 2013, Ojolo et al.[14] presented analytical solutions to the kinetic and heat transfer equations in slow pyrolysis of biomass particles. This is an important phenomenon in the thermochemical conversion process and they represented it with appropriate mathematical models in biomass gasifiers and a pyrolysis reactor. The effects of Biot number, temperature and residence time on particle decomposition are reported.

Heat is transferred to the biomass particle surface from the gaseous surrounding by conduction, convection, and radiation and to the interior by conduction. The temperature inside increases as the heat penetrates more into the interior of the solid, causing moisture evaporation. As the temperature increases above 473 K, the biomass particle decomposes into charcoal, tar and gaseous products up to 723 K after 225 s. At the higher temperature, the rate of thermal decomposition or pyrolysis is not only controlled by heat transfer, but also influenced by heat of reaction, particle shape, air flow rate, and the initial moisture content of the solid fuel.

The kinetic equations of pyrolysis, the heat transfer model and the corresponding initial and boundary condition are given as [14]

$$\frac{\partial C_B}{\partial t} = -(k_1 + k_2 + k_3)C_B, \quad (2.42)$$

$$\frac{\partial C_T}{\partial t} = k_2 C_B - \varepsilon(k_4 + k_5)C_T, \quad (2.43)$$

$$\frac{\partial C_C}{\partial t} = k_3 C_B + \varepsilon k_5 C_T, \quad (2.44)$$

$$\frac{\partial C_G}{\partial t} = k_1 C_B + \varepsilon k_4 C_T, \quad (2.45)$$

where

$$k_i = A_i \exp\left[\frac{-E}{RT}\right]; i = 1, 2, 3, 4, 5. \quad (2.46)$$

The initial condition are

$$t = 0, C_B = C_{B0}, C_C = C_G = C_T = 0. \quad (2.47)$$

The reaction rate coefficient is

$$k_i = A \exp\left[\frac{-E}{R_g T_0}\right] \left(1 + \frac{E}{R_g T_0^2} (T - T_0)\right). \quad (2.48)$$

Where  $C_B$  is the concentration of virgin biomass ( $kg/m^3$ ),  $C_T$  is the concentration of tar ( $kg/m^3$ ),  $C_C$  is the concentration of char ( $kg/m^3$ ),  $C_G$  is the concentration of gas ( $kg/m^3$ ),  $t$  is the time ( $s$ ),  $k_i$  is the rate constant ( $1/s$ ),  $\varepsilon$  is the porosity of the wood particle,  $A$  is the apparent activation energy ( $1/s$ ),  $E$  is the activation energy ( $J/mol$ ),  $R$  is the radius of the particle ( $m$ ),  $T$  is the temperature ( $K$ ),  $T_0$  is the initial temperature ( $K$ ),  $R_g$  is the universal gas constant ( $J/mol$ ).

The heat transfer equation is

$$\rho C_P \frac{\partial T}{\partial t} = K \left[ \frac{\partial^2 T}{\partial r^2} + \frac{1}{r} \frac{\partial T}{\partial r} \right] - Q k_i (\rho - \rho_\infty), \quad (2.49)$$

$$\rho C_P \frac{\partial T}{\partial t} = K \left[ \frac{\partial^2 T}{\partial r^2} + \frac{1}{r} \frac{\partial T}{\partial r} \right] - Q \left( A \exp\left[\frac{-E}{R_g T_0}\right] \left(1 + \frac{E}{R_g T_0^2} (T - T_0)\right) \right) (\rho - \rho_\infty). \quad (2.50)$$

Where  $\rho$  is the bulk density of wood ( $kg/m^3$ ),  $C_P$  is the specific heat capacity ( $J/kgK$ ),  $K$  is the thermal conductivity ( $W/mK$ ),  $r$  is the radial distance ( $m$ ),  $Q$  is the heat of reaction ( $J/kg$ ), and  $\rho_\infty$  is the ultimate density of wood ( $kg/m^3$ ).

The initial and boundary conditions of heat equation are

$$t = 0, T = T_0,$$

$$t > 0, \left(\frac{\partial T}{\partial r}\right)_{r=0} = 0,$$

$$t > 0, -K\left(\frac{\partial T}{\partial r}\right)_{r=R} = h(T_f - T) + \sigma\epsilon(T_f^4 - T^4). \quad (2.51)$$

Where  $R$  is the radius of the particle ( $m$ ),  $h$  is the convective heat transfer coefficient ( $W/m^2 \cdot K$ ),  $T_f$  is the reactor final temperature ( $K$ ),  $\sigma$  is the Stefan Boltzmann constant ( $W/m^2 \cdot K^4$ ), and  $\epsilon$  is the emissivity coefficient.

The concentration of char increases rapidly from 473-673 K and then falls. The temperature history at the center increases, so the Biot number decreases and this temperature is favoured at a Biot number less than 1. The presented paper also compares the result of the heat transfer model with previous work.

## 2.2 Moving Boundary

In 2008, David et al.[5] studied the pyrolysis and combustion of polymers. During these processes, heat is released and a cone calorimeter is used to assess the polymer's flammability. They determined the heat release rate of a one-dimensional transient finite element model using commercial COMSOL Multiphysics software. In this model, the heat and mass transport phenomena taking place throughout the polymer and growing char are considered. This model predicts the heat release rate curve for char forming polymeric material during combustion. In this problem, the partial differential heat and mass transfer equations are coupled together and no analytical solution exists, so that a numerical solution must be sought. In this work, three dimensional transient problem can be simplified to one dimension, which reduces the computation required to solve the system of equations. The physical structure is divided into two regions: the polymer zone and the char formation zone. The char formation zone initially has a length of 1  $mm$  and then grows to 2  $cm$ , where a very thin char layer is introduced, and grows at a velocity corresponding to the rate of pyrolysis.

For mass transfer, the pyrolysis reaction inside the polymer zone is simplified to bring out the essential physics by which polymer goes to gas plus char. This work gives a concentration equation which is the simple model to run in COMSOL Multiphysics,

as follows:

$$r_P = \frac{\partial c_P}{\partial t} = -k_0 \cdot c_P. \quad (2.52)$$

Where  $r_P$  is the rate of polymer consumption during pyrolysis ( $kg/m^3 \cdot s$ ),  $c_P$  is the concentration of polymer ( $kg/m^3$ ),  $t$  is the time ( $s$ ),  $k_0$  is the rate constant for pyrolysis reaction ( $1/s$ ).

Upon heating, the polymer is consumed and gas is produced. Hence, the mass equation of gas can be written as

$$r_{G \circ P} = \frac{\partial c_G}{\partial t} - D_{polymer} \cdot \frac{\partial^2 c_G}{\partial x^2} = \alpha \cdot k_0 \cdot c_P. \quad (2.53)$$

Where  $r_{G \circ P}$  is the rate of gas evolution during pyrolysis ( $kg/m^3 \cdot s$ ),  $c_G$  is the concentration of gases ( $kg/m^3$ ),  $D_{polymer}$  is the diffusion coefficient of gases through polymer ( $m^2/s$ ),  $x$  is the length in the x-direction ( $m$ ), and  $\alpha$  is the mass fraction of gas.

In the case of mass transfer in the char formation zone, when the gas species produced in the polymer zone reaches the char formation zone, it diffuses through the outside boundary to the atmosphere. So, the mass balance in char formation is given by

$$\frac{\partial c_G}{\partial t} - D_{char} \cdot \frac{\partial^2 c_G}{\partial x^2} = 0. \quad (2.54)$$

Where  $D_{char}$  is the diffusion coefficient of gases through char ( $m^2/s$ ).

The polymer is placed in a sample holder and suspended by a thick layer of insulating material and starts off at ambient conditions. For heat transfer, when the polymer is placed under the cone heater, heat is transferred through the polymer by conduction and heat transferred through the surface by radiation. When the gas is produced and diffuses out to the char zone, it can react with oxygen to produce more heat. The heat of volatilization from pyrolysis and other chemical process is given by

$$\rho_{polymer} \cdot C_{P_{polymer}} \cdot \frac{\partial T}{\partial t} - k_{polymer} \cdot \frac{\partial^2 T}{\partial x^2} = -\Delta H_0 \cdot k_0 \cdot c_P + \Delta H_e. \quad (2.55)$$

Where  $\rho_{polymer}$  is the density of polymer ( $kg/m^3$ ),  $C_{P_{polymer}}$  is the heat capacity of polymer ( $J/kg \cdot K$ ),  $k_{polymer}$  is the thermal conductivity of polymer ( $W/m \cdot K$ ),



$C_{P_{polymer}}$  is the heat capacity of char ( $J/kg \cdot K$ ),  $\Delta H_0$  is the of volatilization of polymer ( $J/kg$ ),  $\Delta H_e$  is the heat release or absorbed of in other processes peper.

The heat transfer in char formation zone is described by

$$\rho_{char} \cdot C_{P_{char}} \cdot \frac{\partial T}{\partial t} - k_{char} \cdot \frac{\partial^2 T}{\partial x^2} = 0. \quad (2.56)$$

Where  $\rho_{char}$  is the density of char ( $kg/m^3$ ),  $C_{P_{char}}$  is the heat capacity of char ( $J/kgK$ ),  $k_{char}$  is the thermal conductivity of char ( $W/mK$ ).

At the surface of the char, heat is introduced to the surface by radiation, and leaved the surface to the outside air by convection. Thus, at the surface boundary, the heat flux is given by

$$Q_{surface} = \phi \cdot \Delta H_1 \cdot \left(-\frac{\partial c_G}{\partial x}\right) \Big|_{surface} \cdot D_{char} - h \cdot (T - T_{atm}) + \epsilon \cdot \sigma \cdot (T_{cone}^4 - T^4). \quad (2.57)$$

Where  $Q_{surface}$  is the heat flux at a surface ( $W/m^2$ ),  $\phi$  is the percent heat transferred by heat of combustion,  $\delta H_1$  is the heat of combustion ( $J/mol$ ),  $h$  is the heat transfer coefficient of gas at surface ( $W/m^2 \cdot K$ ),  $T_{atm}$  is the temperature of atmoshere ( $K$ ),  $\epsilon$  is the emissivity,  $\sigma$  is the Stefan-Boltzmann constant ( $W/m^2 \cdot K^4$ ), and  $T_{cone}$  is the temperature of cone heater ( $K$ ).

The heat release rate (HRR) versus time is measured by the heat of combustion and the flux of gas, given by

$$HRR = \Delta H_1 \cdot \left(-\frac{\partial c_G}{\partial x}\right) \Big|_{surface} \cdot D_{char}. \quad (2.58)$$

Where  $HRR$  is the heat release rate ( $W/m^2$ ).

In this work, the moving mesh during char formation is initially set to 1 *nm*. As time proceeds, the polymer heats, the temperature rises, and gas is produced, but ignition does not start until some minimum level of gas surface is reached (minimum level of polymer is lost). When these conditions are reached, ignition begins along with the moving mesh to simulate char formation. In transient numerical modeling, a basic step function cannot be used due to convergence issues. Instead, a smoothed step function is used, where the transition takes place over some given range. In COMSOL Multiphysic, the step function used is called *flc1hs*. Thus, the mesh velocity, *mvel*, can be written



as

$$mvel = flchhs(\rho_{polymer} - c_P|_{x_0} - min, scale) \cdot \frac{(1 - \alpha) \cdot \chi}{\rho_{char}} \cdot \left(-\frac{\partial c_P}{\partial t}\right)|_{x_0}. \quad (2.59)$$

Where  $mvel$  is mesh formation velocity ( $m/s$ ),  $\alpha$  is the fraction of gas and the remaining char, and  $\chi$  is the thickness constant ( $m$ ).

For the solver to use  $(-\frac{\partial c_P}{\partial t})|_{x_0}$  and  $c_P|_{x_0}$  they must be defined in the Extrusion coupling variables and boundary variable section, labelled  $cPt3$  and  $cP3$ , respectively.

From the model, time to ignition and peak heat release rate can be predicted for char forming material by using the computational method. To check the total heat released, the area under the curve of the heat release rate versus time is plotted. The results show the heat release rate from the COMSOL model is compared with the cone data and it is observed that the heat release rates versus time are the same. Thus, the heat release rate curves can be predicted and the cone calorimeter data is not necessary.

Then in 2009, Feyissa et al.[9] studied the heat and mass transfer model with moving boundary during roasting of meat in convection-oven. The model are based on conservation of mass and energy, the formulation of model incorporates the effect of shrinkage phenomena and water holding capacity. The model equations are solved by the finite element method COMSOL Multiphysics. Heat and mass transfer are important role in the roasting process. Heat is supplied to the product surface by convection and transferred from the surface to the center of product mainly by conduction. Liquid water is evaporated at the surface and diffuses to the surrounding fluid which the sample shrinks the surface at water is evaporated changes with time.

In this paper, the conservation of energy is used and then heat transfer within product is assumed to be given by

$$\rho_m c_{P_m} \frac{\partial T}{\partial t} + \nabla(-k_m \nabla T) + \rho_w c_{P_w} u_w \nabla T = 0. \quad (2.60)$$

Where  $\rho_m$  is the density of meat ( $kg/m^3$ ),  $c_{P_m}$  is the specific heat of meat ( $J/kgC$ ),  $T$  is the temperature ( $C$ ),  $t$  is the time ( $s$ ),

For the conservation of mass, the governing equation for water transport inside the product is given as follows,

$$\frac{\partial C}{\partial t} + \nabla(C u_w) = \nabla D \nabla C. \quad (2.61)$$

Where  $C$  is the moisture content ( $kg/s$ ),  $u_w$  is the velocity of water ( $m/s$ ), and  $D$  is the diffusion coefficient ( $m^2/s$ ).

For shrinkage, it is considered that the change of dimensions is proportional to the volume of water removed. The roasting process causes denaturation of proteins in meat which allows for hydration and shrinkage and the simultaneous formation of air filled pore. The following theoretical expressions are formulated.

The interface velocity components can be obtained as:

$$v_z = \frac{dZ}{dt} = -\frac{Z_0\beta}{3V_0} \left(1 - \frac{\beta V_{w,l}}{V_0}\right)^{-2/3} \frac{d}{dt}(V_{w,l}), \quad (2.62)$$

$$v_r = \frac{dR}{dt} = -\frac{R_0\beta}{3V_0} \left(1 - \frac{\beta V_{w,l}}{V_0}\right)^{-2/3} \frac{d}{dt}(V_{w,l}). \quad (2.63)$$

Where  $v_z$  is the length direction velocity ( $m/s$ ),  $v_r$  is the radial direction velocity ( $m/s$ ),  $Z$  is the length ( $m$ ),  $R$  is the radius ( $m$ ),  $V_0$  is the initial volume ( $m^3$ ),  $\beta$  is the shrinkage coefficient, and  $V_{w,l}$  is the volume of water lost ( $m^3$ ).

Finally, the results showing the water content distribution is influenced by the temperature distribution. Inside the meat, the temperature increases when time increases, whereas water content and dimensions are decrease. The temperature increase causes the meat to reduce its water holding capacity and induces shrinkage. The surface of the meat has higher temperature than inside and a large temperature gradient develops from the surface to the inside of product. The meat starts shrinking slowly and the relative change of deformations is reduced. The model can be used to improve the prediction of temperature and moisture loss, it is helpful in understanding the physics of meat in the roasting process.

Although many works studied the mathematical modelling of heat and mass transfer in the process of biomass, but there is no best model. In addition, the torrefaction process is the new technology that increases the efficiency of biomass to bio-coal pellets. The bio-coal is more convenient to use and it is a new evolution of biomass. However fewer studies apply a mathematical model to simulate heat and mass transfer for bio-coal pellets by using COMSOL Multiphysic. Besides this, the simulation of heat and mass transfer couple with free surface movement of a bio-coal is interesting, but there

is no research that has been studied. For this reason, we then try to develop a mathematical model that can simulate heat and mass transfer occurring in the combustion of bio-coal. Moreover, we try to extend our development for a model that can simulate the moving boundary of a bio-coal pellet in the combustion process.



## CHAPTER 3

# HEAT AND MASS TRANSFER OF BIO-COAL PELLETS IN THE COMBUSTION PROCESS

### 3.1 General Overview

Understanding the process and mechanisms involved the combustion of a bio-coal pellet is importance to develop more efficient combustion systems. The process of bio-coal or other products of biomass combustion is extremely complex. Some researchers developed the numerical models for completing the combustion of wood particles or focusing on the specific sub-processes, but this research, we generalized mathematical model for the simulation of a bio-coal degradation, and transference under combustion conditions.

In this research, a mathematical model was developed to simulate the distribution of heat and mass transfer in the combustion process of a bio-coal pellet. Heat and mass transfer occurs on the particle were described by the heat transfer equation coupled with the mass balance equation with appropriate initial and boundary conditions. In this study, we conducted numerical simulations of heat and mass transfer of bio-coal pellet in the combustion process using an algorithm based on the finite element method in the commercial software COMSOL Multiphysics. Moreover, to investigate the effects of the distribution of heat and mass transfer on the pellet in the combustion, we studied some parameters such as thermal conductivity and the specific heat capacity.

There have been many studies of single biomass particle in process and sub-processes of combustion. In 1998, the single solid biomass particle in the pyrolysis was developed which based on physical and chemical changes by Jalan and Srivastava [12]. They

used a finite difference, backward implicit scheme and the 4th order Runge-Kutta predictor corrector method for heat transfer equation and chemical kinetics equation, respectively. In 2003, the single solid particle of biomass in pyrolysis was described by using a mathematical model which presented by Babu and Chaurasia [1]. They coupling the heat transfer and the kinetics equations similarly Jalan and Srivastava [12]. In 2005, mathematical model in the combustion of single wood and thermal degradation of biomass were studied and described by Porteiro [16]. They combines intra-particle combustion with extra-particle transport and use a novel discretisation scheme. Peng et al.[15] studies the effect of particle size of pine on torrefaction and formation of torrefied pellets in thermogravimetric analyzer and tubular fixed bed reactor in 2012. In 2013, analytical solution of heat transfer and kinetic equations of the biomass particle in slow pyrolysis was solved by Ojolo et al.[14]. However, the simulation of heat transfer coupled with mass transfer of bio-coal pellet in the combustion process by using software COMSOL Multiphysic has not yet been investigated.

We, now, firstly introduce the assumptions for this model. Since the bio-coal pellet is a solid, we assume that its properties are constants and independent of temperature. The heat transfer takes place inside the particle by conduction and heat can be locally produced or consumed by combustion. We then also study parameters such as thermal conductivity and the specific heat capacity of a range of materials. This research, the thermal conductivity and heat capacity are constant whereas the rate of volatilization of solid fuel increases with temperature according to Arrhenius law. In the combustion, we assume that the bio-coal was converted to gases, char and tar. Moreover, the temperature gradient at the center line of the solid particle is zero. Finally, we expect the results of the simulation were feasible and reasonable.

In this chapter, we focus on the distribution of heat and mass inside the bio-coal during the combustion. We apply the heat transfer module and mass transport in chemical engineering module in COMSOL Multiphysics to study the behavior or the characteristics of heat and mass at each sides of bio-coal.

The model formulation is given in Section 3.2. The method of solution is presented in Section 3.3. Then, the results and discussion are given in Section 3.4. Finally, some

conclusion are presented in Section 3.5.

### 3.2 Model Formulation

The goal of this research is to study the distribution of heat and the concentration of bio-coal pellet in the combustion process. The process of combustion is very complicated because there are many sub-processes involved such as heating and drying, pyrolysis, and oxidation. We neglect some assumptions to simplify the model. Also, we investigate the effects of the thermal conductivity and heat capacity. The study is based on the assumption that the particle is a solid, which radius  $0.002\text{ m}$  and length  $0.015\text{ m}$ , as shown in Figure 3.1. The particle is contained in a chamber without air and burned only on the bottom for 240 seconds. We assume that heat transfers from the bottom to other surfaces by conduction and radiation, and it transfers into the interior of the particle mainly by conduction. The combustion process is entirely controlled by mixing of fuel species with oxygen. Therefore, the model consists of heat transfer model and mass transfer model.

The model which composes of heat transfer model, mass transfer model, the corresponding initial and boundary conditions are discussed as follows.

Since previous study, Ojolo et al.[14] have been used Eq.(\*), therefore, which is given as follows.

$$\rho C_P \frac{\partial T}{\partial t} = K \left[ \frac{\partial^2 T}{\partial r^2} + \frac{1}{r} \frac{\partial T}{\partial r} \right] - Q_1 \left( A \exp \frac{-E}{RT_0} \left( 1 + \frac{E}{R_g T_0^2} (T - T_0) \right) (\rho - \rho_\infty) \right). \quad (*)$$

Where  $K$  denotes for thermal conductivity ( $W/m \cdot K$ ),  $\rho$  is density ( $kg/m^3$ ),  $\rho_\infty$  is ultimate density ( $kg/m^3$ ),  $C_P$  is specific heat capacity ( $J/kg \cdot K$ ),  $T$  is temperature ( $K$ ),  $T_0$  is initial temperature ( $K$ ),  $A$  is apparent activation energy ( $1/s$ ),  $R$  is radius of the particle ( $m$ ),  $R_g$  is universal gas constant ( $J/mol$ ), and  $Q_1$  is heat of reaction ( $J/kg$ ).

We apply this equation to the heat source term of heat transfer model. The heat transfer equation which we apply is

$$\rho C_P \frac{\partial T}{\partial t} + \nabla \cdot (-k \nabla T) = Q. \quad (3.1)$$

Where  $k$  denotes for thermal conductivity ( $W/m \cdot K$ ) and  $Q$  is the heat source ( $W/m^3$ ).

Therefore, by taking  $Q$  as appears in Eq.(3.1) into the right hand side of Eq.(\*), we have that

$$Q = -Q_1(A \exp^{\frac{-E}{RT_0}} (1 + \frac{E}{R_g T_0^2} (T - T_0)) (\rho - \rho_\infty)). \quad (3.2)$$

The mass balance equation is

$$\frac{\partial c}{\partial t} + \nabla \cdot (-D \nabla c) = R. \quad (3.3)$$

Where  $D$  is a diffusion coefficient ( $m^2/s$ ),  $c$  is the concentration ( $mol/m^3$ ) of bio-coal, and  $R$  is the reaction rate ( $mol/m^3 \cdot s$ ).

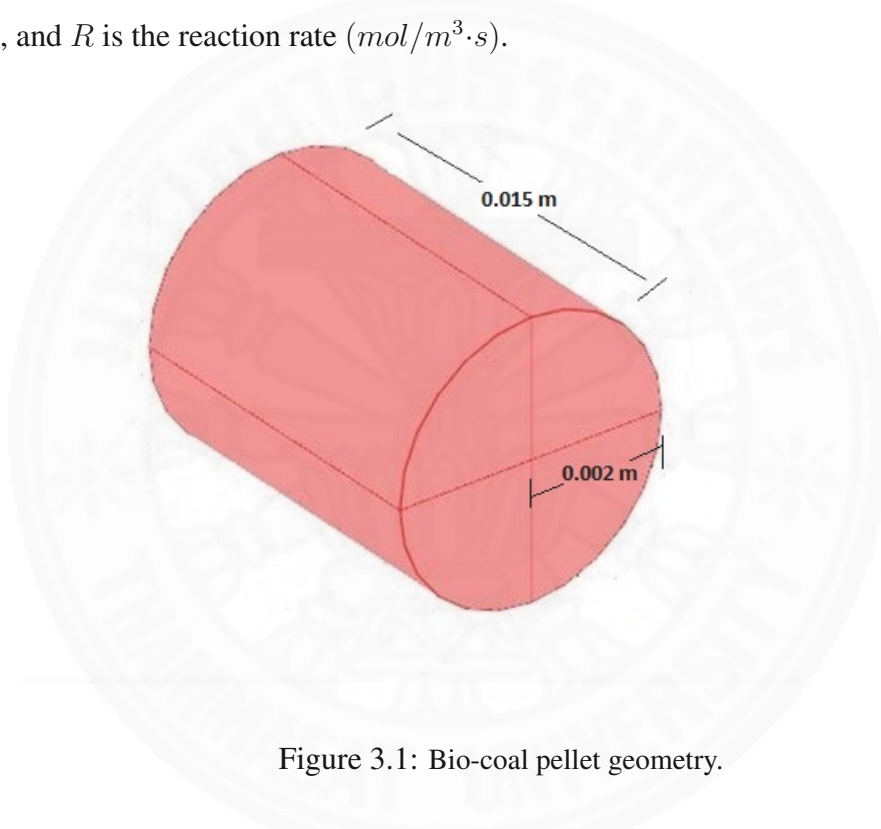


Figure 3.1: Bio-coal pellet geometry.

Since the combustion process is taken place in a chamber with an absence of air, we divide the boundaries of the bio-coal pellet into 3 types: bottom, top, and surface wall. For convenience, when we describe the surface wall, we denote it by the radius  $r = 0.002 m$ .

At the bottom, the initial and boundary conditions are set as follows. The boundary condition at the bottom is set as inward heat flux since it is burned from the outside, as shown in Figure 3.2.

So, the initial condition is

$$t = 0, T = T_0, \quad (3.4)$$

and the boundary condition is

$$t > 0, r = 0.002, -\mathbf{n} \cdot (-k\nabla T) = q_0. \quad (3.5)$$

For the other sides, the boundary conditions are set to radiative heat flux [2, 12, 18] from *surface to ambient* because the assumption that heat is transferred without intermediaries.

So, the initial condition is

$$t = 0, T = T_0, \quad (3.6)$$

and the boundary condition is

$$t > 0, r = 0.002, -\mathbf{n} \cdot (-k\nabla T) = \varepsilon\sigma(T_{amb}^4 - T^4). \quad (3.7)$$

Where  $T_0$  is the initial temperature ( $K$ ),  $q_0$  is the inward heat flux ( $W/m^2$ ),  $\varepsilon$  is the surface emissivity,  $\sigma$  is the Stefan-Boltzmann constant ( $W/m^2 \cdot K^4$ ), and  $T_{amb}$  is the ambient temperature ( $K$ ).

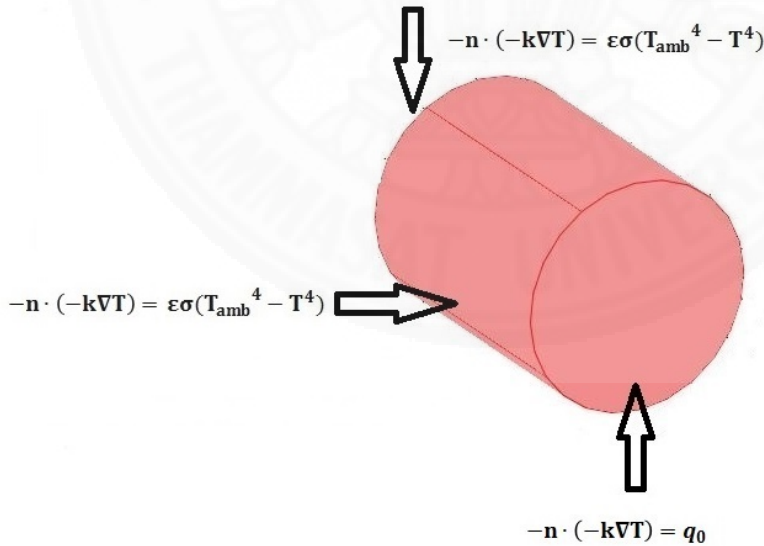


Figure 3.2: Boundary setting of heat transfer on the studied bio-coal pellet.

Similarly, the initial condition for diffusion, the bottom, top, and surface wall of the particle are set to concentration. The boundary condition for diffusion, the bottom, top,



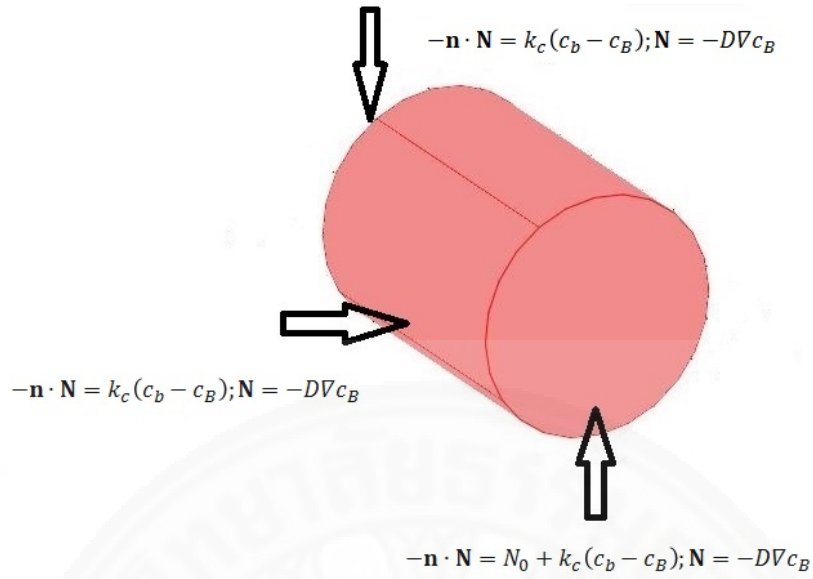


Figure 3.3: Boundary setting of mass transfer on bio-coal pellet.

and surface wall of the particle are set to flux. The boundary condition on the bottom is inward flux, but the other sides are not, because there are not burned, so, the condition are shown as in Figure 3.3. There is no other concentration gradient into the particle.

Thus, the initial condition is

$$t = 0, c = c_0. \quad (3.8)$$

The boundary condition on the bottom is

$$t > 0, r = 0.002, -\mathbf{n} \cdot \mathbf{N} = N_0 + k_c(c_b - c); \mathbf{N} = -D\nabla c, \quad (3.9)$$

and the boundary condition on the other sides is

$$t > 0, r = 0.002, -\mathbf{n} \cdot \mathbf{N} = k_c(c_b - c); \mathbf{N} = -D\nabla c. \quad (3.10)$$

Where  $c_0$  is the initial concentration,  $c_b$  is the bulk concentration ( $mol/m^3$ ),  $N_0$  is the inward flux ( $mol/m^2 \cdot s$ ), and  $k_c$  is the mass transfer coefficient ( $m/s$ ).

### 3.3 Method of Solution

The governing equations in (3.1)-(3.3) and the initial and boundary conditions in (3.4)-(3.10) are coupled to give the initial-boundary value problem (I.B.V.P) of the transient problem of heat and mass transfer.

To solve the problem, we used the finite element method (FEM) in COMSOL Multiphysics. First, we chose 3D in the space dimension and added model navigator as heat transfer module and chemical engineering module. In the application heat transfer module and chemical engineering module, we used transient analysis in general heat transfer and in diffusion, respectively. Then, we went into the draw mode and selected solid style in cylinder. The cylindrical particle in this study was solved with radius 0.002 m and length 0.015 m. Next, set the subdomain and boundary setting by the modeling parameters of heat and mass transfer are given as follows: thermal conductivity  $k = 0.224 \text{ W}/(\text{m} \cdot \text{K})$  [10], density of biomass  $\rho = 650 \text{ kg}/\text{m}^3$  [14], heat capacity  $C_p = 1380 \text{ J}/(\text{kg} \cdot \text{K})$  [7, 16], the heat source  $Q = 9.239178 \times 10^6 \text{ W}/\text{m}^3$  [14], the diffusion coefficient  $D = 1.79 \times 10^{-7} \text{ m}^2/\text{s}$  [1, 2], and the reaction rate  $R = 3.309141 \times 10^8 \text{ mol}/(\text{m}^3 \cdot \text{s})$  [15].

Since the bio-coal pellet is assumed to be burned on the bottom at all times, therefore the heat flux also flows into the particle over time as well. In addition, at the starting of ignition, the temperature is 311 K. Over a period of four minutes, the temperature increases to 473 K. Hence we set the inward heat flux to  $q_0 = -8.4 \times (311 + (t \times 7.883) - T) \text{ W}/\text{m}^2$ . The other system parameters of heat and mass transfer are as follows: surface emissivity  $\varepsilon = 0.95$  [12, 14], the Stefan-Boltzmann constant  $\sigma = 5.67 \times 10^{-8} \text{ W}/(\text{m}^2 \cdot \text{K}^4)$  [1, 2, 10, 14], the ambient temperature  $T_{amb} = 311 \text{ K}$ , the inward flux  $N_0 = -1.3 \text{ mol}/(\text{m}^2 \cdot \text{s})$ , the mass transfer coefficient  $k_c = 2 \times 10^{-3} \text{ m}/\text{s}$  [3], and the bulk concentration  $c_b = 650 \text{ mol}/\text{m}^3$  [14].

Before solving the problem, we set the mesh mode by dividing the domain into a collection of subdomains, with each subdomain represented by a set of element, which has tetrahedral 8482 elements and the number of mesh points has 1738 nodes as shown in Figure 3.4. Finally, we solved the problem with the absolute tolerance and the relative tolerance of the solver parameters of  $10^{-7}$  and  $10^{-6}$ , respectively. For solving each time,

the linear system solver of UMFPACK was chosen.

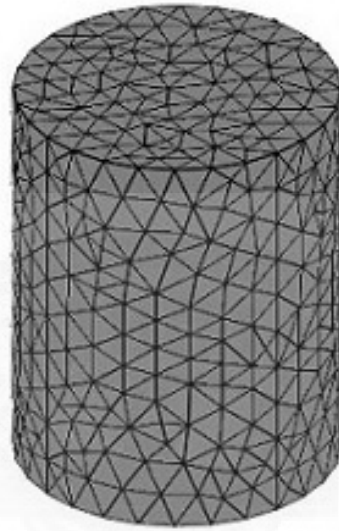


Figure 3.4: Finite element mesh of 8482 Lagrange order one tetrahedral element with 1738 nodes

### 3.4 Numerical Results and Discussion

In the present work, we study the heat and mass transfer of bio-coal in combustion process with the dimensions shown in Figure 3.1. The model is solved for a particle with radius 0.002 m and length 0.015 m. For the results, we shows the surface, arrow, and slice plot of temperature distribution and concentration. For the slice plot, we can set the data into cross-section plot parameter which shows about plane and inside of bio-coal.

To investigate the influence of the materials on the heat and mass transfer, we simulate heat and mass transfer for different values of heat capacity  $C_p$  and thermal conductivity  $k$ . We simulate for  $C_p = 1380 \text{ J}/(\text{kg} \cdot \text{K})$ ,  $C_p = 1726 \text{ J}/(\text{kg} \cdot \text{K})$  [7, 11],  $k = 0.311 \text{ W}/(\text{m} \cdot \text{K})$ , and  $k = 0.185 \text{ W}/(\text{m} \cdot \text{K})$  [10].

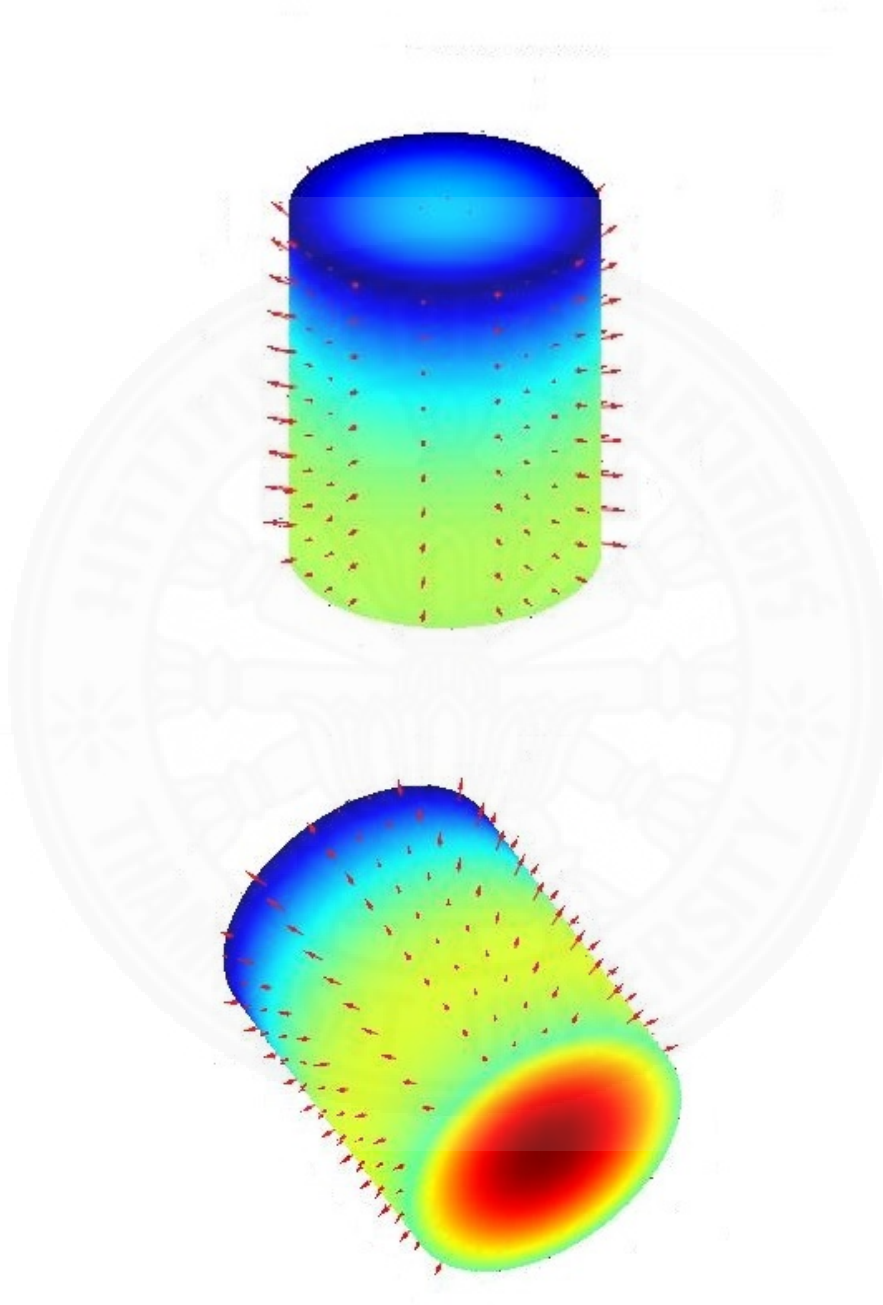


Figure 3.5: Arrow and surface plots of heat transfer of the bio-coal pellet

Figure 3.5 and Figure 3.6 shows arrow and surface plots of heat and mass transfer in the bio-coal pellet. It can be seen that the heat flux flows from the burned bottom of the bio-coal pellet to the top and the surface wall. Similarly to heat flow, the concentration of pellet transfer from the bottom to another sides.

Figure 3.7 and Figure 3.8 shows the slice plots of heat and mass transfer at heat capacities  $C_p = 1380 \text{ J}/(\text{kg} \cdot \text{K})$  and  $C_p = 1726 \text{ J}/(\text{kg} \cdot \text{K})$ . For each value of heat capacity at each time, heat is transferred from the burned bottom upwards and to the other sides, as shown in Figures 3.7(a<sub>1</sub>) – 3.7(a<sub>3</sub>) and Figures 3.8(a<sub>1</sub>) – 3.8(a<sub>3</sub>).

At time  $t$ , we can observe that the highest temperature occurred along the center of the bio-coal pellet. We can also see that a rapid temperature increase during the first time period. For example in a layer at times,  $t = 120\text{s}$  and  $t = 240\text{s}$ , the temperatures were 619.829 K and 624.493 K, respectively. The temperature then fell.

The simulations of mass transfer are shown in Figures 3.7(b<sub>1</sub>) – 3.7(b<sub>3</sub>) and Figures 3.8(b<sub>1</sub>) – 3.8(b<sub>3</sub>). At the time  $t = 240\text{s}$ , the concentration was in the range 36.827 to 649.969  $\text{mol}/\text{m}^3$ . As time progressed, the concentration at the burned bottom of the bio-coal decreased more than in other areas.

At each time, the mass of bio-coal in the burned area decomposed and escaped the burned side, moving toward the pellet to other areas in the same pattern as the heat distribution.

We can see that when the heat capacity increased from 1380 to 1726  $\text{J}/(\text{kg} \cdot \text{K})$ , the temperature increased from the range [590.842-656.978] to [591.098-657.783] K. Hence a high heat capacity transferred more temperature than a low heat capacity.

Figure 3.9 and Figure 3.10 shows the slice plot of heat and mass transfer at thermal conductivities of  $k = 0.311 \text{ W}/(\text{m} \cdot \text{K})$  and  $k = 0.185 \text{ W}/(\text{m} \cdot \text{K})$ , respectively. We observe that the heat and mass transfer was similar to those obtained in different values of heat capacity.

At the same point in the pellet, at a thermal conductivity of  $k = 0.311 \text{ W}/(\text{m} \cdot \text{K})$ , and  $k = 0.185 \text{ W}/(\text{m} \cdot \text{K})$  the temperature was 625.125 K, and 624.393 K, respectively. We observe that a higher thermal conductivity can conduct a higher temperature more lower thermal conductivity.

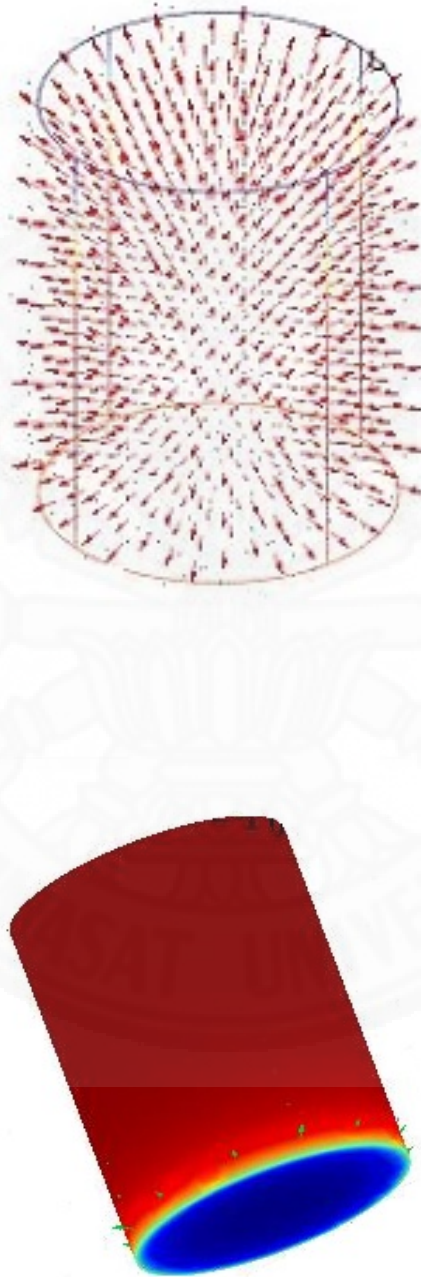


Figure 3.6: Arrow and surface plots of mass transfer of the bio-coal pellet

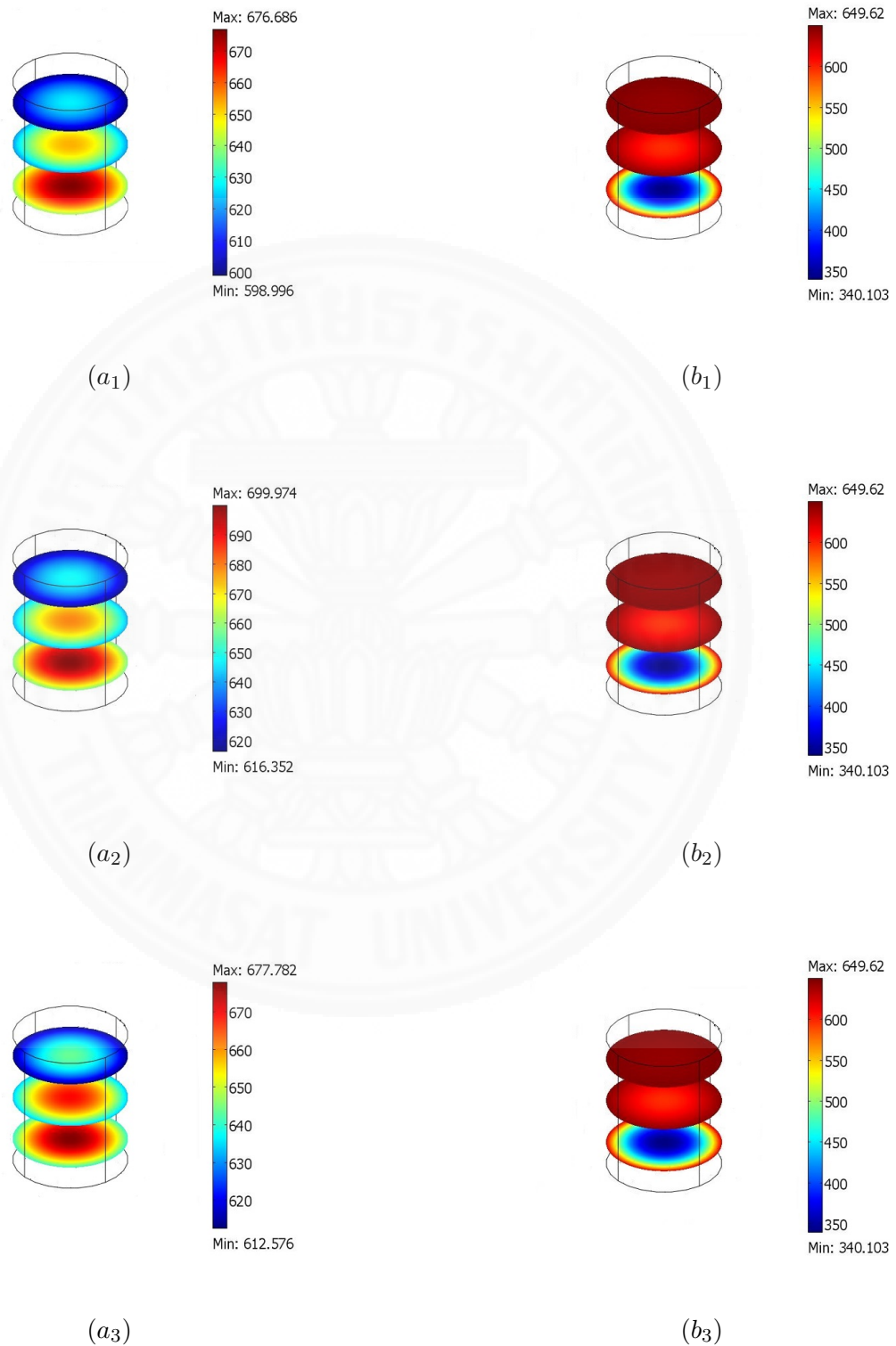


Figure 3.7: Slice plots of heat transfer  $(a_1)–(a_3)$  and mass transfer  $(b_1)–(b_3)$  when  $C_p = 1380$   $J/(kg \cdot K)$  at  $t=30s, 120s, \text{ and } 240s$ .



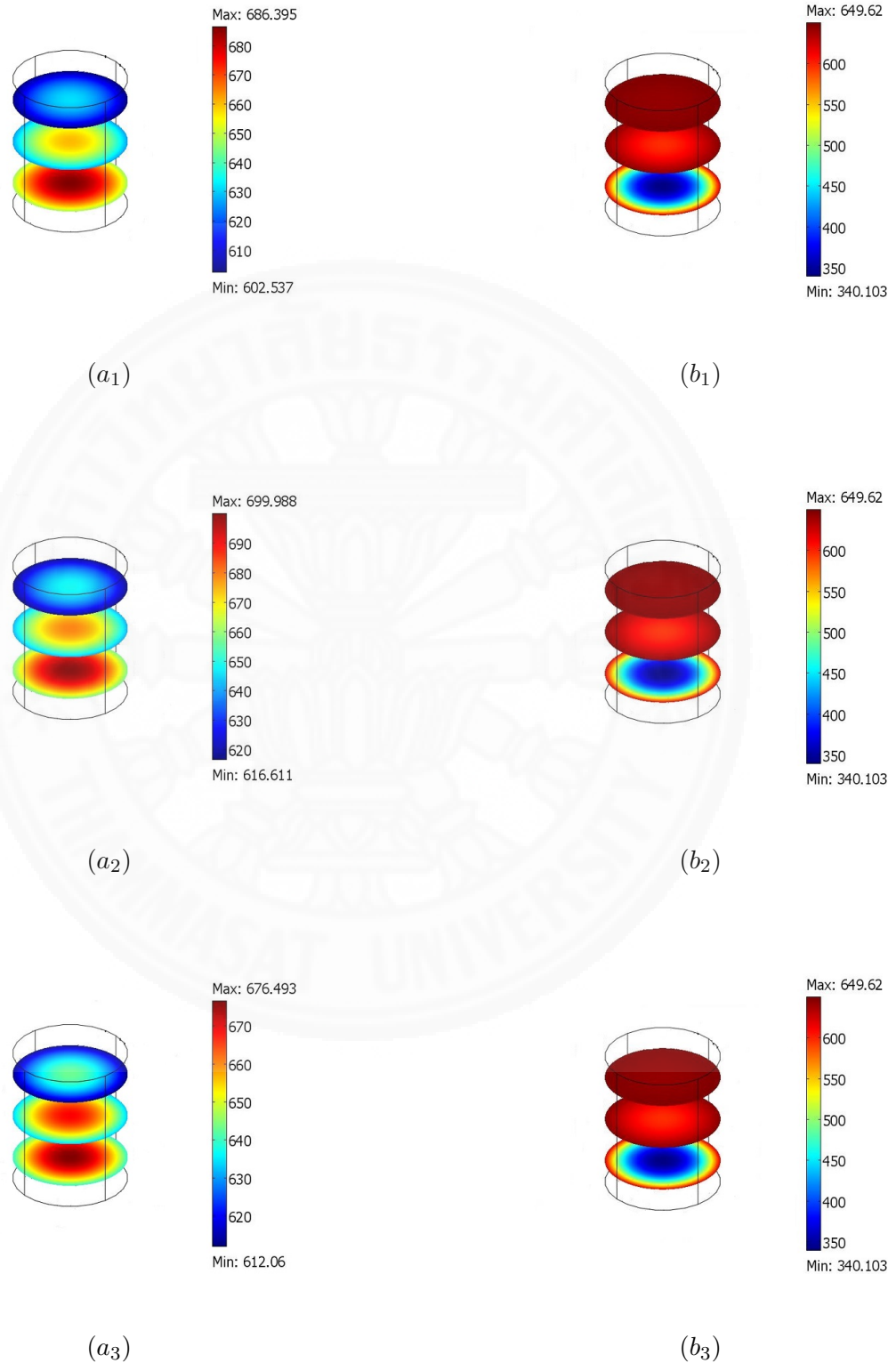


Figure 3.8: Slice plots of heat transfer  $(a_1) - (a_3)$  and mass transfer  $(b_1) - (b_3)$  when  $C_p = 1726$   $J/(kg \cdot K)$  at  $t=30s, 120s,$  and  $240s$ .



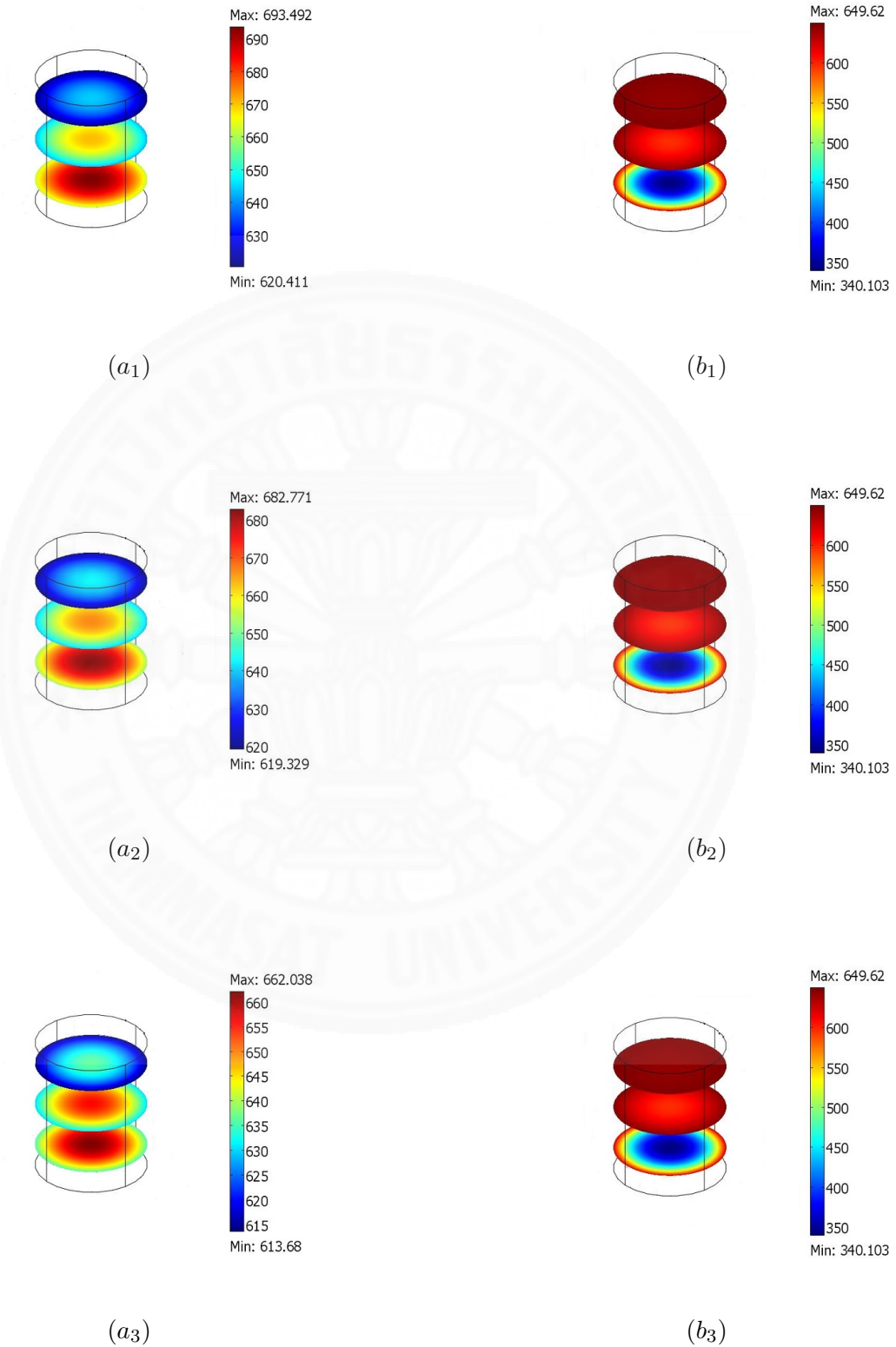


Figure 3.9: Slice plots of heat transfer  $(a_1) - (a_3)$  and mass transfer  $(b_1) - (b_3)$  when  $k = 0.311$   $W/(m \cdot K)$  at  $t=30s, 120s,$  and  $240s$  .

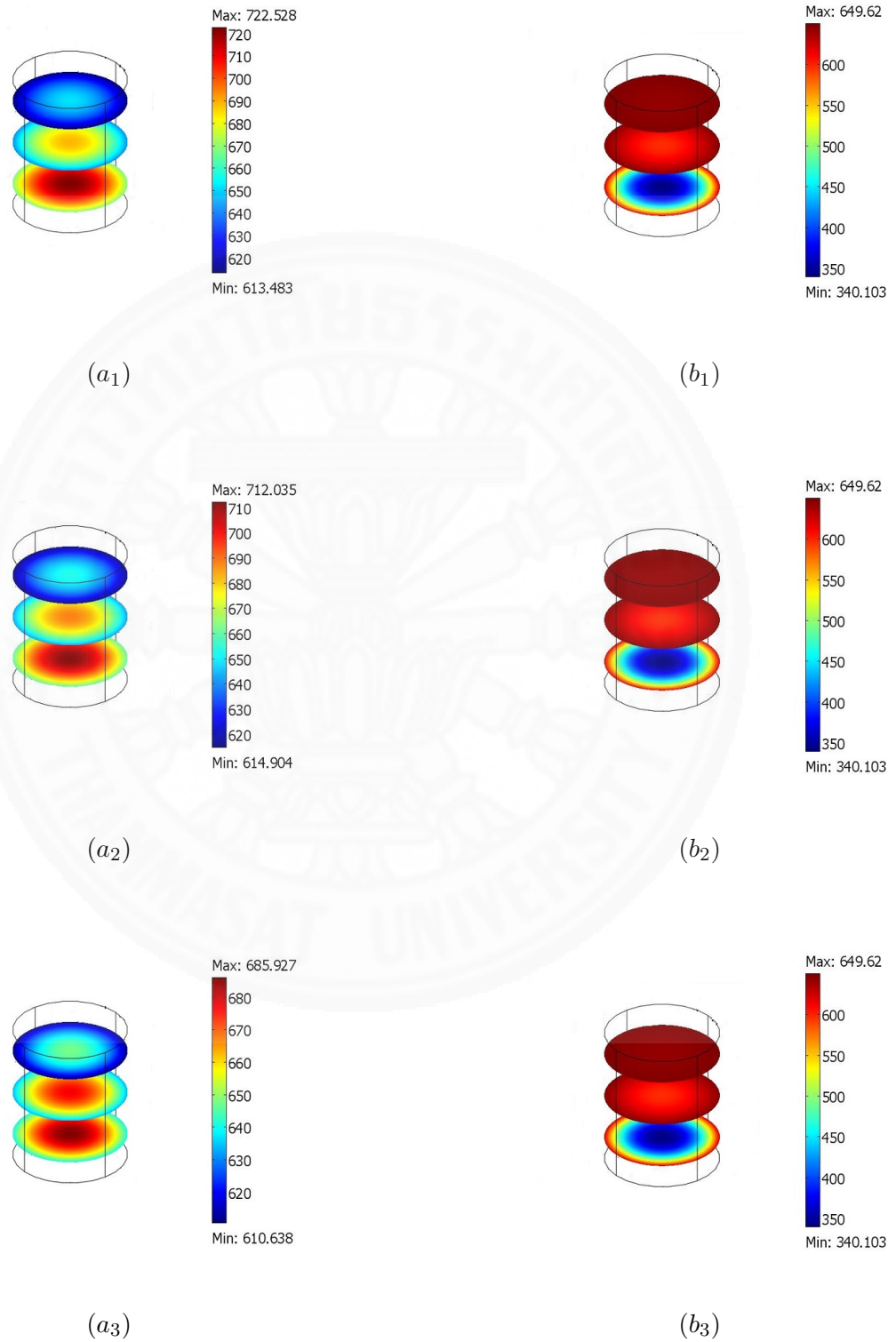


Figure 3.10: Slice plots of heat transfer  $(a_1) - (a_3)$  and mass transfer  $(b_1) - (b_3)$  when  $k = 0.185 W/(m \cdot K)$  at  $t=30s$ ,  $120s$  and  $240s$  .

### 3.5 Conclusion

A mathematical model for simulating the distribution of heat and mass transfer in the combustion process of a bio-coal pellet has been developed, combining the heat transfer equation with the mass balance equation. Numerical simulation is then used to investigate the effects of the material parameters on the heat and mass transfer of the pellet.

The study shows that the highest temperature occurs along the center of the pellet. The temperature increases rapidly during the first time period. On the burned bottom, the concentration more decrease than in other areas. The heat spread to the top and surface wall, the concentration shows the same pattern as the temperature. Using different values of heat capacity and thermal conductivity, we demonstrate that a high heat capacity and high thermal conductivity can conduct a higher temperature than low heat capacity and low thermal conductivity. The results are reasonable and in agreement with previous work [1, 12].

## **CHAPTER 4**

### **THE COMBUSTION OF BIO-COAL PELLETS WITH BOUNDARY MOVEMENT**

#### **4.1 General Overview**

To analyze and improve the quality of the bio-coal pellets, it is important to understand the contraction of the burning surface. Likewise, the transient of heat and mass transfer with free surface movement of a bio-coal pellet in the combustion is also very interesting. Many approaches have been used to simulate the reaction of heat and mass on a biomass pellet, but there is no approach has been simulated heat and mass transfer on a bio-coal with moving free surface.

The Arbitrary Lagrangian-Eulerian method (ALE) is commonly used for simulating deforming computation domains. It applies a structural computation to adjust the local shape of the free surface or interface. It is first used in fluid mechanics and has been successfully applied to finite element analysis in solid mechanics. The ALE technique combines a fixed mesh (Eulerian) and a moving mesh following the material deformation (Lagrangian) by introducing a new computational mesh that can be fixed or can be moved [6]. This method is appropriate to use with a structured computational grid which deforms during the solution procedure.

Even fewer studies have considered the boundary movement on a solid particle in the combustion process, though studies have been made of surface movement in a polymer during pyrolysis and combustion. In 2008, a finite element analysis was used to model the heat release rate, as assessed by a cone calorimeter of a char forming polycarbonate, by David et al.[5]. They used the moving mesh in COMSOL Multiphysics

to study the char formation related to heat and concentration of particles. Besides, in 2009, a mathematical model of heat and mass transfer was developed by taking into account the shrinkage effect for meat roasting in a convection oven by Feyissa et al.[9]. The model equations describing coupled heat and mass transfer with moving boundary were solved using chemical engineering module and moving mesh module in COMSOL Multiphysics. However, the coupled heat and mass transfer with boundary movement of a bio-coal in the combustion process has not yet been investigated.

Since biomass fuels are primarily composed of oxygen, carbon, and hydrogen, the main products from burning biomass are carbon dioxide and water. Heat and mass transfer phenomena within the bio-coal particle during combustion cause gases to be produced or mass to be lost, and then change the structural of particle. To study the structural changes, it is important to take the free surface movement or moving boundary into account in the model of burning bio-coal.

In this chapter, we focus on the change of shape for a cylindrical bio-coal particle with a moving boundary and the reaction involved in the combustion. We apply the ALE finite element technique in COMSOL Multiphysics to study the dynamics of the deformation of a burning bio-coal. The model formulation is presented in Section 4.2. The method of solution is given in Section 4.3. The results and discussion are presented in Section 4.4. Finally, some points of conclusion are given in Section 4.5.

## **4.2 Model Formulation**

We start this section by describing the assumed situation of combustion process as follows. First, a cylindrically shaped bio-coal is placed in a small furnace (small chamber) that has only one side opened that is called the fire-door. We assume that the bio-coal is attached to the wall of the furnace at the opposite side of the fire-door. For other sides of the bio-coal, they are surrounded by small cavity to the chamber walls.

The bio-coal starts off at the ambient conditions. Then the bio-coal is first heated by radiation from the outsource fire at the fire-door, say the bottom. As the bottom side heats, the bio-coal begin to break down into smaller gas molecules. The small gases then diffuse out of the sample particle and into the atmosphere below the side where the

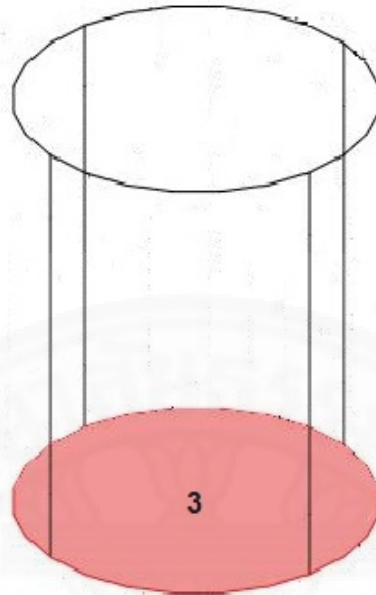


Figure 4.1: The sides of bio-coal pellet in 3 dimensions

air is presented. These gases then react with the oxygen in the air, and thus, the combustion occurs. In this situation, we assume that the heat transfers throughout within the particle by conduction. We also assume that during the combustion, the volatile gases are released as carbon monoxide ( $CO$ ), carbon dioxide ( $CO_2$ ), and methane ( $CH_4$ ), and the volume of gas produced affected the mass of the bio-coal. Therefore, we consider the initial reaction of gases and ignored the char by coupling the concentration of gas to the model. As we can see from the situation, the structure of the bio-coal, especially on the burned side, must change all time in the combustion process.

However the mathematical modeling of the combustion for bio-coal pellets with a moving boundary has been little studied, we assume a simple model to explain the phenomena. Three application modes coupled in the time-dependent problem consists of (1) heat transfer model, (2) mass transfer model and (3) moving boundary model (ALE).

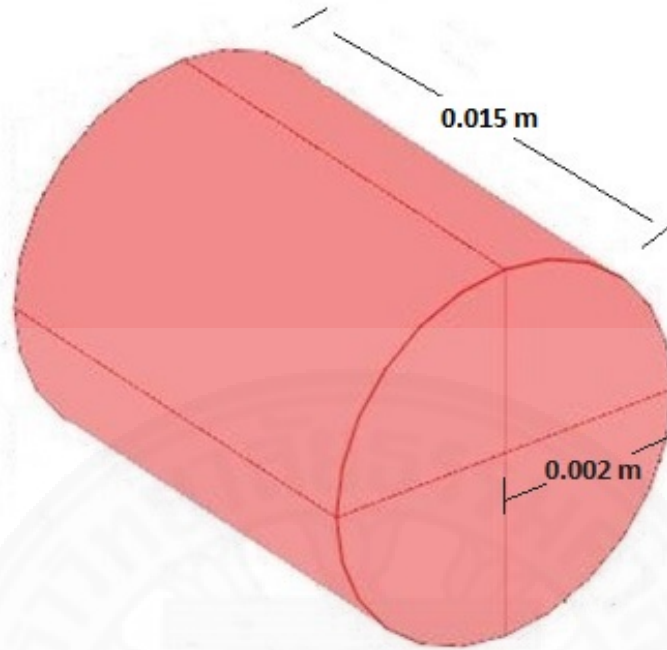


Figure 4.2: The size of bio-coal pellet in 2 and 3 dimensions

#### 4.2.1 Heat Transfer

Since we assume that the heat transfer throughout within the particle by conduction and transfers to the surface by radiation. We can describe the situation for the heat transfer as follows.

##### Heat Transfer in Bio-Coal Pellet Zone

In the bio-coal zone, heat transfers by conduction. The heat equation from combustion and the heat from other chemical processes are given by

$$\rho C_P \frac{\partial T}{\partial t} + \nabla \cdot (-k \nabla T) = Q, \quad (4.1)$$

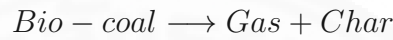
where  $k$  is thermal conductivity ( $W/m \cdot K$ ),  $\rho$  is density ( $kg/m^3$ ),  $C_P$  is heat capacity ( $J/kg \cdot K$ ),  $T$  is temperature ( $K$ ), and  $Q$  is heat source ( $W/m^3$ ). So, the parameter  $Q$  is represented as the previous chapter.

$$Q = -Q_1 \left( A \exp^{\frac{-E}{RT_0}} \left( 1 + \frac{E}{R_g T_0^2} (T - T_0) \right) (\rho - \rho_\infty) \right). \quad (4.2)$$

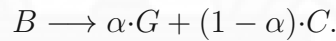
Where  $\rho$  is density ( $kg/m^3$ ),  $\rho_\infty$  is ultimate density ( $kg/m^3$ ),  $T$  is temperature ( $K$ ),  $T_0$  is initial temperature ( $K$ ),  $A$  is apparent activation energy ( $1/s$ ),  $R$  is radius of the particle ( $m$ ),  $R_g$  is universal gas constant ( $J/mol$ ), and  $Q_1$  is heat of reaction ( $J/kg$ ).

#### 4.2.2 Mass Transfer

The reaction inside the bio-coal is shown as:



or



Upon heating, the bio-coal breaks down into char and gas. Preliminary, we study the gas reaction only and the effect of char is not consider. The bio-coal accounts for the combustion reaction; bio-coal is consumed and gases are produced.

During this reaction, the mass of the bio-coal is consumed to produce a fraction  $\alpha$  of gas. The first order reaction rate for bio-coal mass consumption is given by

$$\frac{\partial m_B}{\partial t} = -k_0 \cdot m_B, \quad (4.3)$$

where  $m_B$  is the mass of the bio-coal ( $kg$ ),  $t$  is time ( $s$ ), and  $k_0$  is the rate constant for the combustion reaction ( $1/s$ ).

The used rate constant  $k_0$  is a function of temperature which can be described by the Arrhenius relationship:

$$k_0 = A_0 \cdot \exp\left[\frac{-E_{A0}}{R \cdot T}\right]. \quad (4.4)$$

Where  $A_0$  is the pre-exponential factor of the combustion reaction ( $1/s$ ),  $E_{A0}$  is the activation energy of the combustion reaction ( $kJ/mol$ ), and  $R$  is the gas constant ( $J/mol \cdot K$ ).

Considering the physics of the problem, the bottom must move to the left as particle is consumed. In the model, it is assumed that the computational domain which



composes of bio-coal zone and gas zone. Thus the volume is constant while the concentration changes with time. We divide both sides by a constant volume, giving a concentration equation which is easier to work with in COMSOL Multiphysics. Thus we can re-write the concentration equation:

$$r_B = \frac{\partial c_B}{\partial t} = -k_0 \cdot c_B. \quad (4.5)$$

Therefore, our concentration equation for bio-coal in this software version is:

$$\frac{\partial c_B}{\partial t} + \nabla \cdot (-D_B \nabla c_B) = R. \quad (4.6)$$

Then, we have

$$r_B = -k_0 \cdot c_B = R. \quad (4.7)$$

Where  $r_B$  is the rate of bio-coal consumption during pyrolysis ( $kg/m^3 \cdot s$ ),  $R$  is the reaction rate ( $mol/m^3 \cdot s$ ), and  $c_B$  is the concentration of bio-coal ( $kg/m^3$ ).

When the bio-coal is consumed during the reaction, gas is produced. Therefore, the mass balance on the gas species that is produced is given by

$$r_G = \frac{\partial c_G}{\partial t} - D_B \cdot \frac{\partial^2 c_G}{\partial x^2} = \alpha \cdot k_0 \cdot c_B. \quad (4.8)$$

In the same way, the model of the diffusion of gas in this software is

$$\frac{\partial c_G}{\partial t} + \nabla \cdot (-D_G \nabla c_G) = R, \quad (4.9)$$

so,

$$r_G = \alpha \cdot k_0 \cdot c_B = R. \quad (4.10)$$

Where  $r_G$  is the rate of gas evolution during pyrolysis ( $kg/m^3 \cdot s$ ),  $c_G$  is the concentration of gases ( $kg/m^3$ ),  $D_B$  is the diffusion coefficient of pyrolysis gases through bio-coal ( $m^2/s$ ),  $x$  is length in the x-direction ( $m$ ), and  $\alpha$  is the mass fraction of gas that is produced.

### 4.2.3 Moving Mesh (ALE)

Since we are interested in the situation which the pellet is burned on one side, we define a change in the ignition side. Inside the model, each subdomain is set to free displacement, in which the mesh is not fixed in each subdomain but it can move. The mesh displacement is constrained only by the boundary conditions on the surrounding boundaries. On the top and the side wall, the mesh displacement is set to zero, meaning that it is fixed in space. Since we consider only the side that is burned and we are interested in only the gases produced, so the mesh growth velocity on the bottom must be set with the rate of mass growth. It is important to recognize the governing phenomena that control this complex system.

To find the mesh velocity at the bottom, the rate of mass growth for gas or the rate of mass reduction for bio-coal can be equated as:

$$\frac{\partial m_G}{\partial t} = -\alpha \frac{\partial m_B}{\partial t} = \alpha \cdot k_0 m_B, \quad (4.11)$$

where  $m_G$  is the mass of gas ( $kg$ ) and  $m_B$  is the mass of bio-coal ( $kg$ ).

Dividing both sides by  $\rho_{gas}$ , we obtain that on the left side becomes

$$\frac{1}{\rho_{gas}} \frac{\partial m_G}{\partial t} = \frac{\partial \left( \frac{m_B}{\rho_{gas}} \right)}{\partial t} = \frac{\partial V}{\partial t} = \frac{\partial Ax}{\partial t} = A \frac{\partial x}{\partial t}, \quad (4.12)$$

where  $\rho_{gas}$  is the density of gas ( $kg/m^3$ ),  $V$  is the volume,  $A$  is the area, and  $x$  is the displacement of gas.

Then, we have

$$A \frac{\partial x}{\partial t} = -\frac{\alpha}{\rho_{gas}} \frac{\partial m_B}{\partial t} = \frac{\alpha \cdot k_0}{\rho_{gas}} m_B. \quad (4.13)$$

Dividing both sides by  $A$  and multiplying both denominator and numerator of the right hand side by a constant thickness  $\chi$ , the distance between the top and the bottom of the bio-coal, 15 mm, gives

$$\frac{\partial x}{\partial t} = -\frac{\alpha \cdot A \cdot \chi}{\rho_{gas} \cdot \chi} \frac{\partial m_B}{A \partial t} = \frac{\alpha \cdot k_0 \cdot \chi}{\rho_{gas}} \frac{m_B}{A \cdot \chi}. \quad (4.14)$$

Recognizing that  $(A \cdot \chi)$  is a constant volume,  $m_B/A \cdot \chi = c_B$  and  $m_G/(A \cdot \chi) = c_G$ , the mesh velocity  $mvel$ , can be defined as

$$mvel = \frac{\partial x}{\partial t} = -\frac{\alpha \cdot \chi}{\rho_{gas}} \frac{\partial c_B}{\partial t} = \frac{\alpha \cdot k_0 \cdot \chi}{\rho_{gas}} c_B. \quad (4.15)$$

For the modeling purposes, the rate of concentration of bio-coal ( $\frac{\partial c_B}{\partial t}$ ) is then used and is specified at a particular boundary. Here  $c_B$  is zero at the boundary where gas growth. Therefore, the mesh velocity becomes

$$mvel = \frac{\alpha \cdot \chi}{\rho_{gas}} \cdot \left(-\frac{\partial c_B}{\partial t}\right). \quad (4.16)$$

Where  $mvel$  is the mesh formation velocity ( $m/s$ ) and  $\chi$  is the thickness constant at the top to the bottom ( $m$ ). Even though this value is small, its effect on the heat and mass transfer is enough to produce significant effect on the results.

This function should only become active when  $c_G$  reaches the minimum level of gas surface concentration for ignition and the minimum level of bio-coal loss. If this happens at all times, then gas growth would be taking place from the very beginning.

To solve the mesh velocity in COMSOL Multiphysics, we define ( $-\frac{\partial c_B}{\partial t}$ ) in the Extrusion Coupling Variables and Boundary Variables section. The name created cBt3 is given to the bottom. On this boundary, we set the general transformation by source transformation and set selected boundaries as destination transformation which equal to Y.

#### 4.2.4 Initial and Boundary Conditions

The initial conditions for each boundary can be defined as follows.

At  $t = 0$ , we have

$$T = T_0, \quad (4.17)$$

$$c_B = c_0 = \rho, \quad (4.18)$$

$$c_G = 0. \quad (4.19)$$

For the boundary conditions, we divide into 3 zones: top, side wall and bottom.

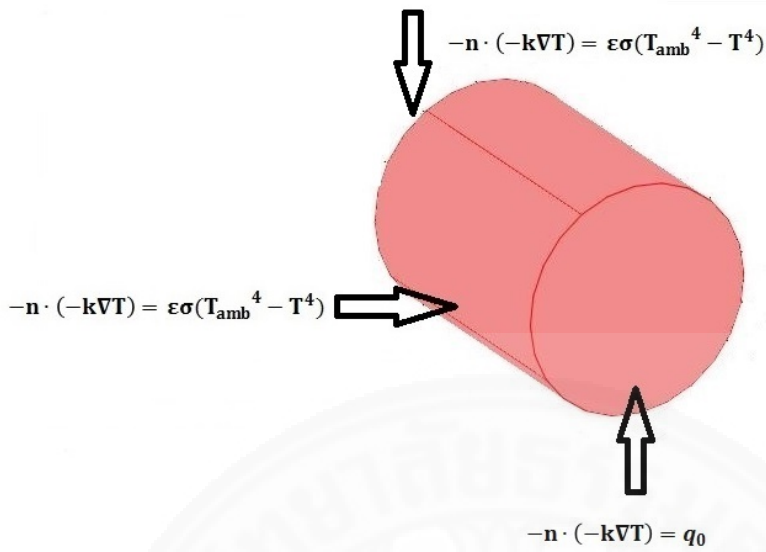


Figure 4.3: The boundary condition of heat transfer model of bio-coal pellet.

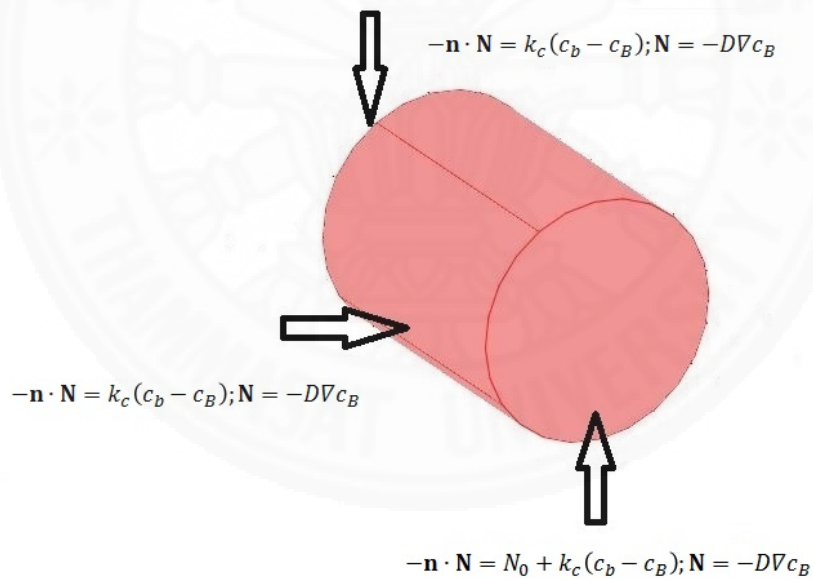


Figure 4.4: The boundary condition of mass transfer model of bio-coal pellet.

**On the top of bio-coal:** We assume that in this area is not burned directly, so we set heat flux into radiation type that is *surface to ambient* as show in Figure 4.3. The concentration of bio-coal and gas are set to flux as shown in Figures 4.4 and 4.5, re-

spectively. For moving mesh on this side, we set a mesh velocity which is zero value in all directions, because we assume that it would not be burned and is unlikely to be affected within the time limit. Thus, the boundary conditions on the top are as follows.

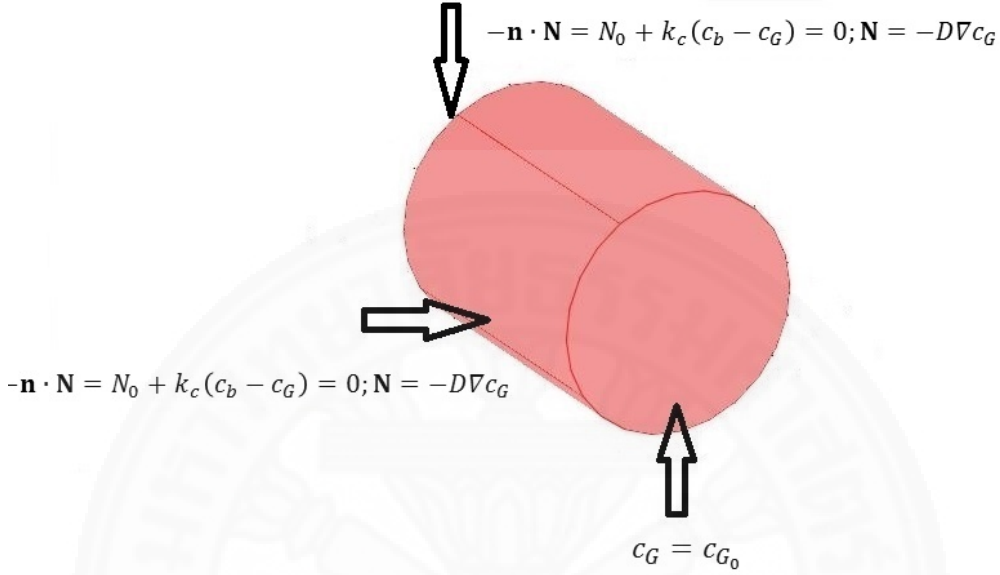


Figure 4.5: The boundary condition of mass transfer model of gas.

The boundary condition of heat transfer is given by

$$t > 0, \quad -\mathbf{n} \cdot (-k\nabla T) = \epsilon\sigma(T_{amb}^4 - T^4). \quad (4.20)$$

The boundary condition of mass transfer of bio-coal is given by

$$t > 0, \quad -\mathbf{n} \cdot \mathbf{N} = k_c(c_b - c_B); \mathbf{N} = -D_B\nabla c_B. \quad (4.21)$$

The boundary condition of mass transfer of gas is given by

$$t > 0, \quad -\mathbf{n} \cdot \mathbf{N} = N_0 + k_c(c_b - c_G) = 0; \mathbf{N} = -D_G\nabla c_G. \quad (4.22)$$

The boundary of the moving mesh were set as follows:

$$v_x = 0, v_y = 0, \text{ and } v_z = 0. \quad (4.23)$$

**On the surface of the side wall:** We set the boundary conditions as same as to the top.

**On the burned bottom side:** At this side of the bio-coal, heat is introduced by radiation and some of this heat may be reflected back. The bottom is burned and heated directly, so we set an inward heat flux for the heat transfer model and flux for mass transfer of bio-coal as shown in Figure 4.3 and Figure 4.4. The mass transfer model of the gas is set by using the concentration as shown in Figure 4.5, and the moving mesh is defined by the mesh velocity.

The boundary condition of heat transfer is given by

$$t > 0, \quad -\mathbf{n} \cdot (-k \nabla T) = q_0. \quad (4.24)$$

At this boundary, the heat flux entering the surface is described by

$$q_0 = Q_{surface} = \phi \cdot \Delta H_1 \cdot \left(-\frac{\partial c_G}{\partial x}\right) \cdot D_B - h \cdot (T - T_{atm}) + \epsilon \cdot \sigma \cdot (T_{amb}^4 - T^4). \quad (4.25)$$

where  $q_0$  is inward heat flux ( $W/m^2$ ),  $Q_{surface}$  is heat flux at the surface ( $W/m^2$ ),  $\phi$  is the heat transferred by the heat of combustion, it is given as a percentage,  $\Delta H_1$  is the heat of combustion ( $J/mol$ ),  $h$  is the heat transfer coefficient of the gas at the surface ( $W/m^2 \cdot K$ ),  $T_{atm}$  is the temperature of the atmosphere ( $K$ ),  $\epsilon$  is emissivity,  $\sigma$  is the Stefan-Boltzmann constant ( $W/m^2 \cdot K^4$ ), and  $T_{amb}$  is the ambient temperature ( $K$ ).

For convenience in modeling, the convection heat loss term can be combined with the heat of combustion term, eliminating a parameter that is not exactly known. It is easy to adjust parameter  $\phi$ , which means the percentage of heat which is transferred back to the surface [5].

The boundary condition of mass transfer of bio-coal is given by

$$t > 0, \quad -\mathbf{n} \cdot \mathbf{N} = N_0 + k_c(c_b - c_B); \quad \mathbf{N} = -D \nabla c_B. \quad (4.26)$$

The boundary condition of mass transfer of gas is given by

$$t > 0, \quad c_G = c_{G_0}. \quad (4.27)$$

The boundary condition of the moving mesh is given by

$$v_x = \frac{(c_B t_3 * \alpha)}{\rho_{gas}},$$

$$vy = \frac{(cBt3 * \alpha)}{\rho_{gas}},$$

$$vz = \frac{(cBt3 * \alpha)}{\rho_{gas}}. \quad (4.28)$$

Where  $T_0$  is the initial temperature ( $K$ ),  $\epsilon$  is surface emissivity,  $\sigma$  is the Stefan-Boltzmann constant ( $W/m^2 \cdot K^4$ ),  $T_{amb}$  is ambient temperature ( $K$ ),  $N_0$  is inward flux ( $mol/m^2 \cdot s$ ),  $k_c$  is the mass transfer coefficient ( $m/s$ ),  $c_b$  is the bulk concentration ( $mol/m^3$ ),  $c_G$  is the concentration of gas ( $mol/m^3$ ),  $vx$  is mesh velocity in the x-direction ( $m/s$ ),  $vy$  is mesh velocity in the y-direction ( $m/s$ ), and  $vz$  is mesh velocity in the z-direction ( $m/s$ ).

### 4.3 Method of Solution

The governing equations for heat and mass transfer of bio-coal and mass transfer of gas in (4.1)-(4.10) with initial and boundary conditions in (4.17)-(4.27) are coupled to be the initial boundary value problem (I.B.V.P). To observe the change of shape, we couple the boundary value problem with the boundary movement in (4.23) and (4.28). It means that we now have the model for bio-coal with a moving boundary. The model is solved for the pellet which has radius 0.002 m and length 0.015 m. The modeling parameters on the subdomain of heat and mass transfer and the moving boundary are as follows. For heat and mass transfer, the values of the parameters are the same as in the previous chapter for thermal conductivity ( $k$ ), the density of biomass ( $\rho$ ), the heat capacity ( $c_p$ ), and the reaction heat ( $R$ ), but the diffusion coefficient is set as  $D = 0$ .

Since the features of the combustion is similar to those previously studied, the parameters on the boundary for surface emissivity ( $\epsilon$ ), the Stefan-Boltzmann constant ( $\sigma$ ), the ambient temperature ( $T_{amp}$ ), the inward flux ( $N_0$ ), the mass transfer coefficient ( $k_c$ ), and the bulk concentration are the same as shown in Chapter 3. On the burned bottom part of the bio-coal, the inward heat flux ( $q_0$ ), is constructed from (4.25). Hence, the inward heat flux is  $q_0 = 0.2 * 210000 * (-\frac{\partial c_G}{\partial x}) * 1.79 * 10^{-7} - (8.4 * (311 + (t * 7.883) - T))$ .

The modeling parameters on the subdomain and boundary of mass transfer of gases are set as follows. The diffusion coefficient  $D = 1.79 * (10^{-7})$  [1, 2] and the rate of

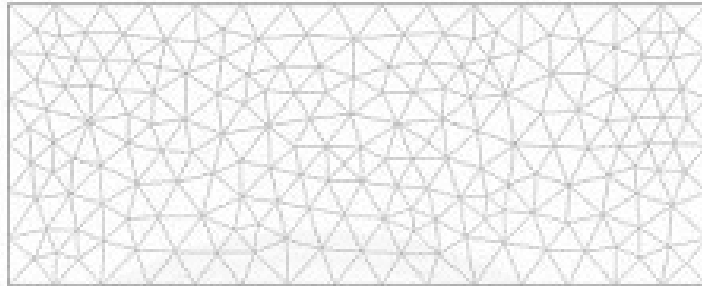


Figure 4.6: Finite element mesh of 374 Lagrange order one tetrahedral element with 209 nodes in 2 dimensions.

reaction is opposite to the reaction rate of bio-coal. That is, the reaction rate of gas is

$$R = A * \exp\left(\frac{-E}{Rg*T}\right) * c.$$

For the model of the moving mesh, we set the subdomain to free displacement and the burned side to mesh velocity. In this boundary, we follows the work [5], where  $vx$ ,  $vy$ , and  $vz$  are equal to  $\frac{cBt^3 \cdot \alpha}{\rho_{gas}}$ . Since this boundary is continuously burned, it has changed with the time.

To solve the problem, the finite element method in COMSOL Multiphysics is used. The domain of the problem is divided into subdomains, each of which subdomain represents a set of elements. The 2D case has a triangular arrangement 374 elements, and the 3D has a tetrahedral arrangement of 6445 elements as shown in Figure 4.6-4.7. For the number of mesh point, this model has 209 nodes in 2D and 1588 nodes in 3D. We solve the problem in a maximum time of 240 second and observe the different phenomena at each time. For the solver parameters, the absolute tolerance is set to  $10^{-7}$  and the relative tolerance is set to  $10^{-8}$ . The used linear system solver for solving each time step, we selected UMFPAK.



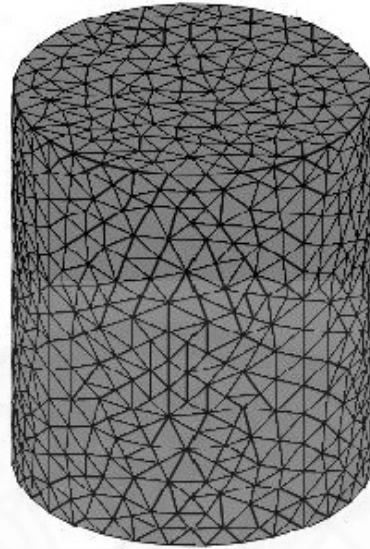


Figure 4.7: Finite element mesh of 6445 Lagrange order one tetrahedral element with 1588 nodes in 3 dimensions.

#### 4.4 Results and Discussion

In the present work, we study the heat and mass transfer of bio-coal by combining the mass transfer of the gas product and the moving mesh in the combustion.

To demonstrate the behavior of heat and mass transfer and change of shape which is affected by gas growth or the concentration of bio-coal, the finite element method COMSOL Multiphysics is able to estimate the results and present them in the form of arrow and surface plots. This commercial software can simulate and show the distribution of heat and mass inside the bio-coal at each time with the transformation of boundary.

Figure 4.8 and Figure 4.9 shows the arrow and surface plots of heat transfer in 2D and 3D, respectively, which has been affected by gases produced. We can see that the heat flux flows from the burned side toward to the top and the side wall.

Since we set the running time to 240 seconds, at this time, the temperature was between 1042.996 and 1181.807 K. At each time, we observe that the temperature increases gradually, in the earliest stage and then slowly declines.

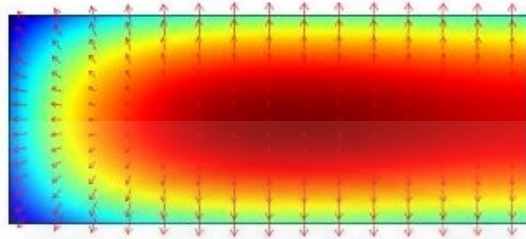


Figure 4.8: The arrow plot of heat transfer in 2 dimensions.

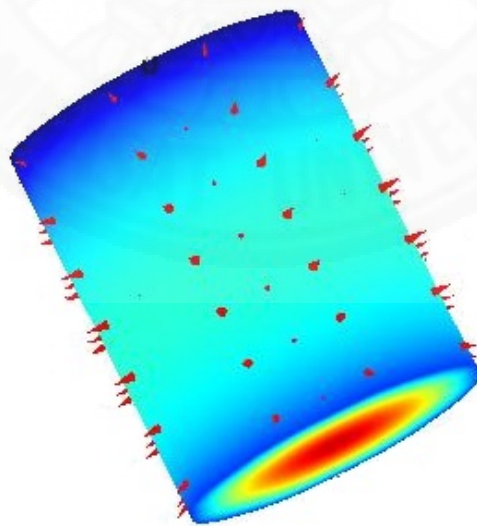


Figure 4.9: The arrow plot of heat transfer in 3 dimensions.

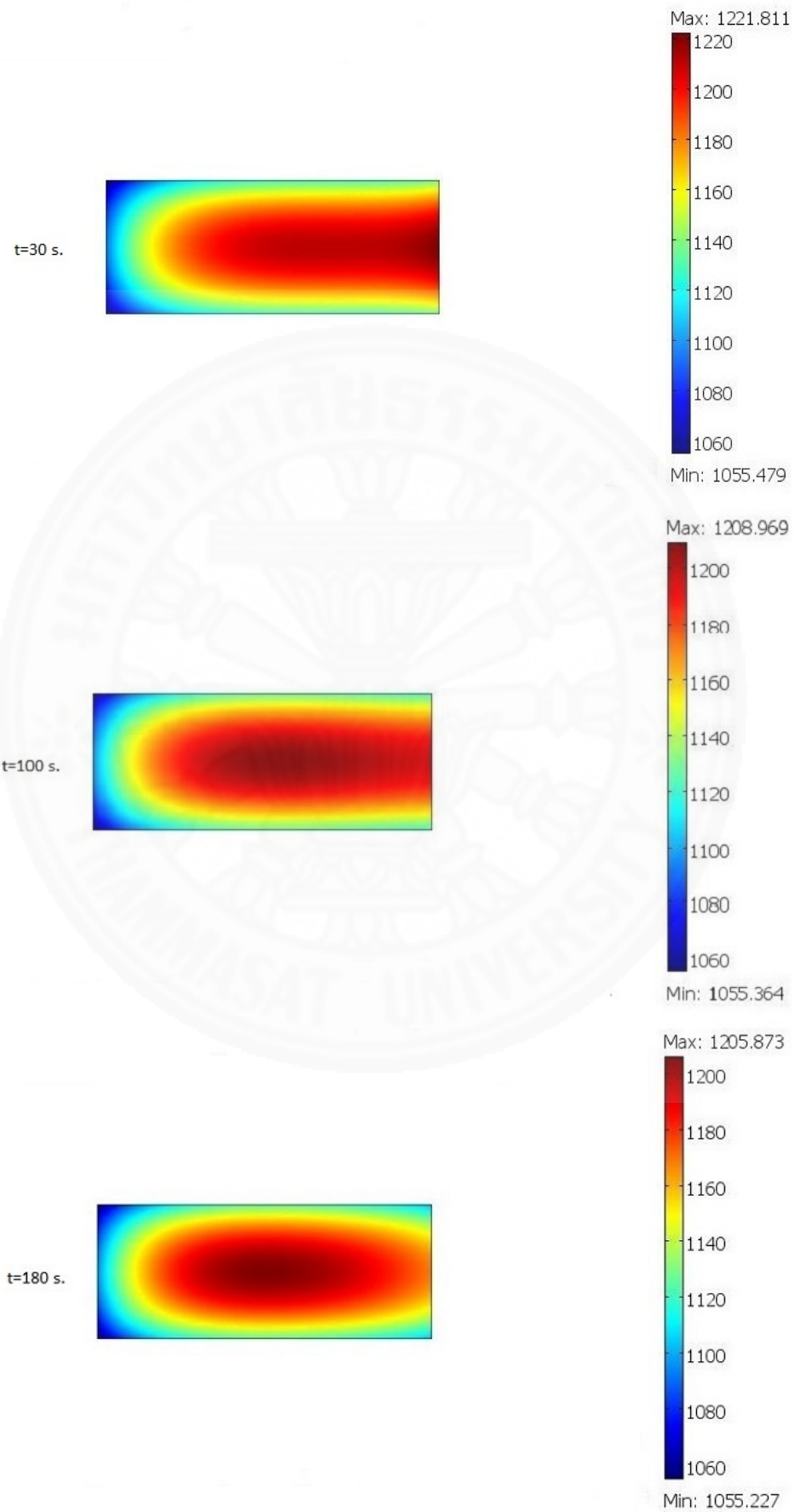


Figure 4.10: The heat transfer in 2 dimensions at time=30s, 100s and 180s.

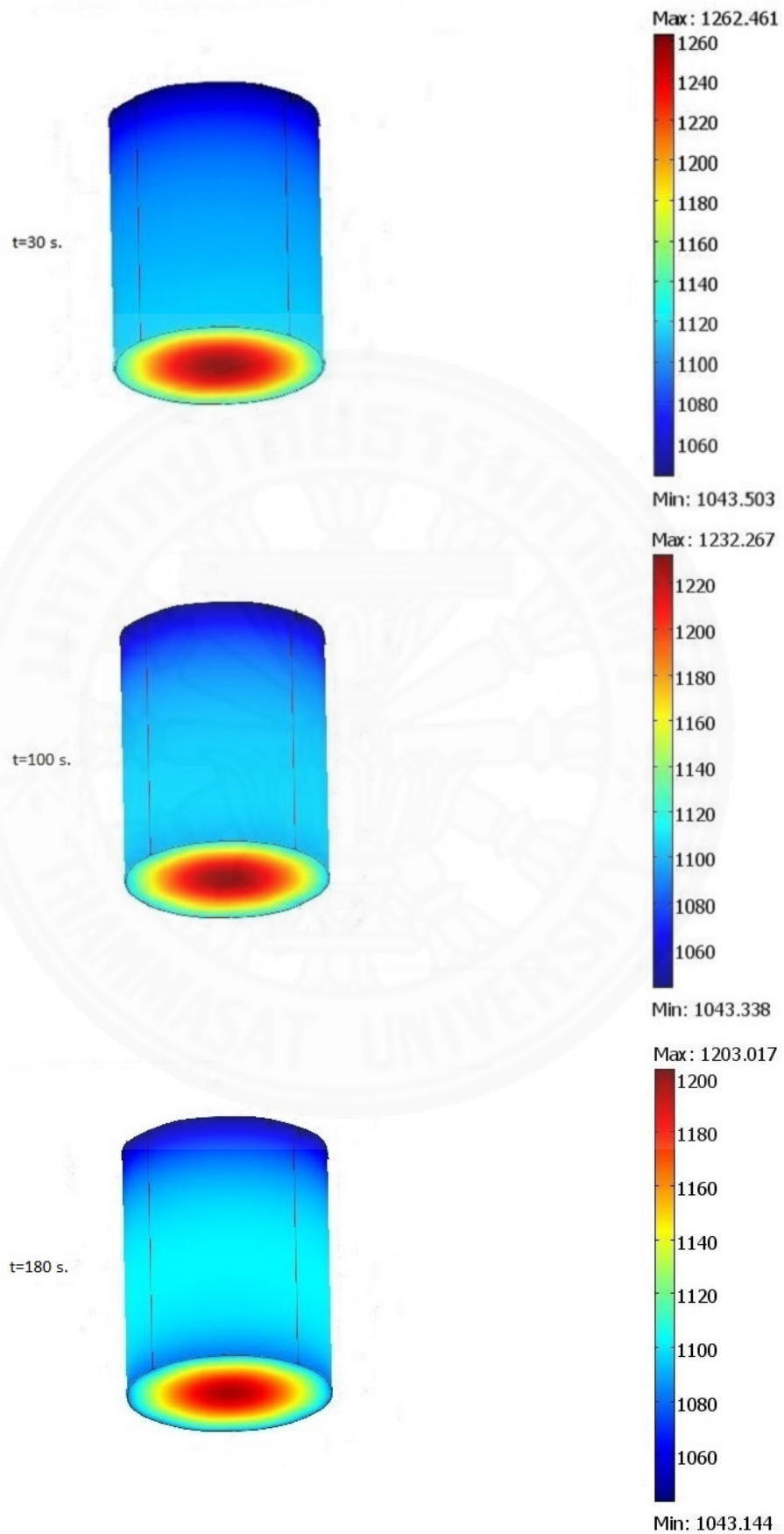


Figure 4.11: The heat transfer in 3 dimensions at time=30s, 100s and 180s.

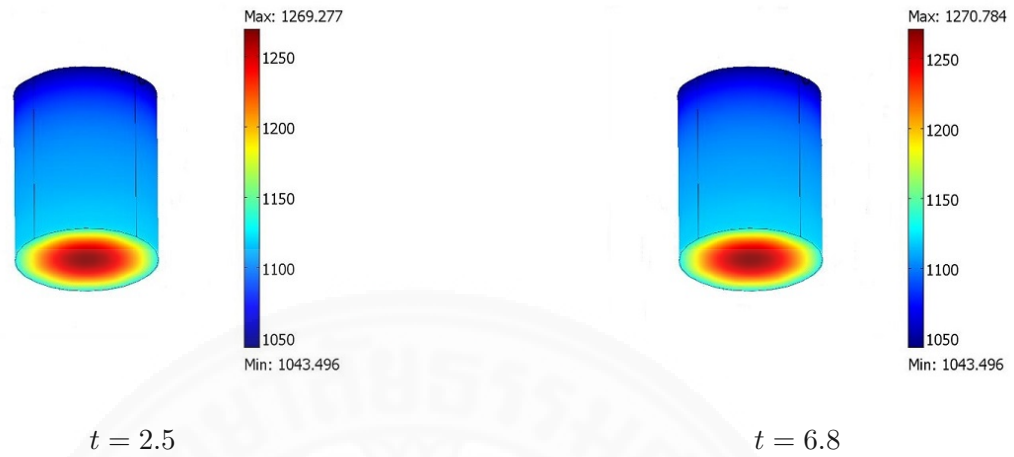


Figure 4.12: The heat transfer at  $t=2.5s$  and  $6.8s$ .

As time passed, the temperature at the bottom more drop because the effect of the loss of mass and gas growth. Hence, this area uses less heat and then the higher temperature spreads to the area which without mass loss. Figure 4.10 and Figure 4.11 shows the temperature at different time, for example,

- 2D At  $t = 30s.$ , the temperature range is 1055.479 to 1221.811 K.  
 At  $t = 100s.$ , the temperature range is 1055.364 to 1208.969 K.  
 At  $t = 180s.$ , the temperature range is 1055.227 to 1205.873 K.
- 3D At  $t = 30s.$ , the temperature range is 1043.503 to 1262.461 K.  
 At  $t = 100s.$ , the temperature range is 1043.338 to 1232.267 K.  
 At  $t = 180s.$ , the temperature range is 1043.144 to 1203.017 K.

The temperature at the bottom increases until the time equal to 6.8 second which the maximum temperature is 1270.784 K as show in Figure 4.12, then fall slightly as heat moves into other areas and temperature at the central part becomes highest.

As time progresses, the bio-coal produces heat and as the temperature rises, gas is produced. The level of gas surface concentration is such that the whole mass of the bio-coal is lost, the ignition front moves to simulate the contraction of the bio-coal.

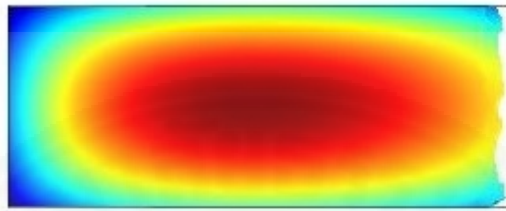


Figure 4.13: Deformation in 2 dimensions.



Figure 4.14: Deformation in 3 dimensions.

Figures 4.13 and Figure 4.14 shows the subdomain deformation of bio-coal in 2 dimensions and 3 dimensions, respectively. We can observe that the concentration of bio-coal decreases rapidly. It means that mass of the bio-coal is gradually dissipating and causing the physical changes. Over time, at the burned side, the frame of the pellet shrinks slightly as the figures.

#### **4.5 Conclusion**

Now, a sophisticated mathematical model for heat and mass transfer with moving boundary of a bio-coal in the combustion process has been constructed. We also have investigated the temperature changes associated with gas growth or the loss in concentration of bio-coal. The results of our simulation shows that the temperature inside the bio-coal gradually increased in the first period and then declined slightly. In the reaction, as gas is produced, the concentration of bio-coal decreases and the temperature changes. The highest temperature occurs along the center of the bio-coal and the temperature in each area for each different time.

For the physical form of the bio-coal, we found that from the start of burning to the final time, the burned side shrink. The concentration at the burned side decreases rapidly more than in other areas, causing the contraction.

Therefore, we conclude that the model of heat transfer and mass transfer with a moving boundary proved accurate and satisfactory. The developed model would be useful to study the behavior that occurs during the combustion of bio-coal.

## CHAPTER 5

### SUMMARY AND CONCLUSIONS

This research focus on the development of two mathematical models including of the numerical simulation of heat and mass transfer model and the model of heat and mass transfer couple with boundary movement of bio-coal pellets in the combustion process. The purposes of the first model is to study the distribution behavior of heat and mass in bio-coal during the combustion. The second model intend to study the structural change of shape at the burned side by using of moving boundary. The ALE technique is used to deal with the moving coordinate system. Numerical algorithms based on the finite element method and the ALE finite element method in the COMSOL Multiphysics have been developed for solving two problems. Therefore, the obtained results from both models are summarized as follows.

#### **5.1 The simulation of heat and mass transfer of bio-coal.**

First, mathematical model describes the distribution of heat and mass in bio-coal by using heat transfer equation and mass balance equation. Although the heat transfer equation is used in many research but it is often coupled with the kinetics equation. For this research, the heat transfer equation is coupled with the mass balance equation of bio-coal and considered the transfer behavior in transient state. Since we study the bio-coal pellet in cylindrical shape in the combustion process which is very complicated, we use a simple model by making some assumptions or neglecting something but it can still explain the phenomena well. The obtained results are concluded as follows.

(a) Both fluxes of the heat and mass are transferred from the burned bottom to the top and the side wall. The heat spreads to the top and sides which the concentration is the same pattern.



(b) The temperature inside the pellet increases rapidly during the first time period and then the temperature a little bit drop. The highest temperature occurs along the center of the pellet. For the mass transfer, the concentration on the bottom decreases than other areas. Then, the concentration of bio-coal is decomposed more rapidly at the burned side than other areas.

(c) Using the two different values of heat capacity and thermal conductivity as defined in Section 3.4, we obtain the similar dissemination pattern that is heat is transferred from the bottom to upward and to other sides. The high heat capacity and high thermal conductivity conduct a higher temperature more than low heat capacity and low thermal conductivity.

## **5.2 The simulation of free surface movement coupled with heat and mass transfer model.**

In the second part, a mathematical model has been presented to explain the behavior of the structural change of shape when the bio-coal is burned in the chamber without air. Under the assumption that while burning the pellet, heat and mass are transferred, gas is produced and mass is consumed. In this case, we do not consider the char growth but discuss the gas product or gas reaction only. We observe that the temperature and the heat transfer are affected by the gas growth. Then, we analyzed the changes of mass and shape of bio-coal. To simulate the free surface movement and solve the problem, we used technique ALE and finite element method in COMSOL Multiphysics. The conclusions are as follows.

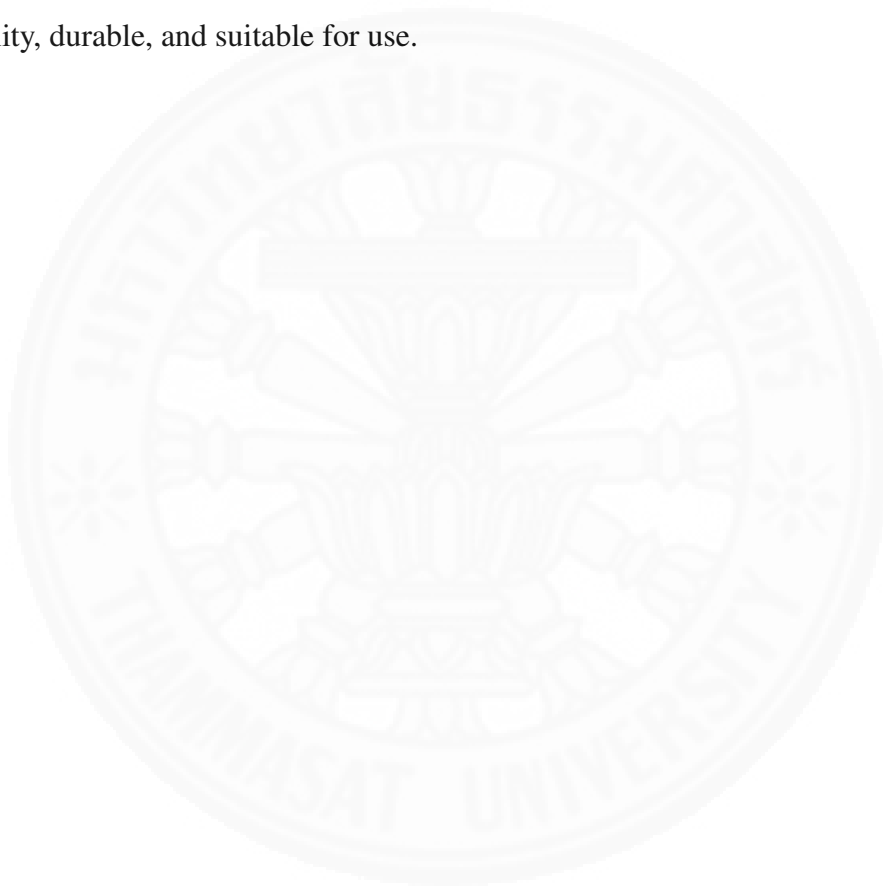
(a) The heat flux flows from the burned bottom toward the top and the side wall. In the first time period, the temperature increases until its peak, increases until 6.8 second and then slowly down. The heat moves to other areas and the highest temperature occurs along center of pellet. This results are similar to the characteristics of heat transfer occurring in Chapter 3.

(b) As the gas reaction is produced, it makes the concentration or the mass of bio-coal decreases and this effect to the changing of temperature.

(c) In the combustion process, the physical shape has changed by the burned side shrink slightly which means that the concentration decreases more than in other areas

causing to the contraction of bio-coal.

(d) This research presents an analysis of the heat and mass transfer and the shrinkage behavior of a bio-coal. The results provide the information and knowledge to be applied and optimized of a bio-coal pellet in the combustion process. Moreover, if the model is developed by studying more realistic situation and some properties are defined as close to reality even more which is useful to study the behavior of heat dissipation and shrinkage of the bio-coal. That is this development allows us to improve a bio-coal quality, durable, and suitable for use.



## REFERENCES

- [1] Babu BV, Chuarasia AS. Modeling for pyrolysis of solid particle kinetics and heat transfer effects. *Energy Conversion and Management*, 2002;44:2251-2275.
- [2] Babu BV, Chuarasia AS. Pyrolysis of biomass:improved models for simultaneous kinetics and transport of heat, mass and momentum. *Energy Conversion and Management*, 2003;45:1297-1327.
- [3] Brito AG, and Melo LF. Mass transfer coefficients within anaerobic biofilms: effects of external liquid velocity. *Wat.Res*, 1999;33:3673-3678.
- [4] Comsol.com. Multiphysics: What is mass transfer, COMSOL Inc.2016.
- [6] Donea J, Arbitrary Lagrangian-Eulerian Methods. *Encyclopedia of Computational Mechanics*, John Wiley and Sons 2004.
- [5] David L. Statler Jr, and Rakesh K. Gupta. A finite element analysis on the modeling of heat release rate, as assessed by a cone calorimeter, of char forming polycarbonate. Boston, 2008.
- [7] Dupont C, Chiriac R, Gauthir G, and Toche F. Heat capacity measurement of various biomass types and pyrolysis residues. *Fuel*, 2014;115:644-651.
- [8] Ferrero F, Malow M, Berger A, and Krause U. Modelling the coupled heat and mass transfer during fires in stored biomass, coal and recycling deposits. Berlin:

Germany, 2007.

- [9] Feyissa A.H, Adler-Nissen J, and Gernaey K.V. Model of heat and mass transfer with moving boundary during roasting of meat in convection-oven. Milan, 2009.
- [10] Guo W, Lim JC, Sokhansanj S, and Melin S. Determination of effective thermal conductivity and specific heat capacity of wood pellets. *Fuel*, 2013;103:347-366.
- [11] Gupta M, Yang J, and Roy C. Specific heat and thermal conductivity of softwood bark and softwood char particle. *Fuel*, 2003;82:919-927.
- [12] Jalan PK, Srivastava VK. Studies on pyrolysis of single biomass cylindrical pellet-kinetic and heat transfer effects. *Energy Conversion and Management*, 1999;40:467-494.
- [13] Lu H, Robert W, Peirce G, Ripa B, and Baxter LL. Comprehensive study of biomass particle combustion. *Energy & Fuels*, 2008;22:2826-2839.
- [14] Ojolo SJ, Osheku CA, and Sobamowo MG. Analytical investigation of kinetic and heat transfer in slow pyrolysis of a biomass particle. *Int. Journal of Renewable Energy Development*, 2013;2(2):105-115.
- [15] Peng JH, Bi HT, Sokhansanj S, and Lim JC. A study of particle size effect on biomass torrefaction and densification. *Energy & Fuels*, 2012;26:3826-3839.
- [16] Porterio J, Miguez JL, Granada E, and Moran JC. Mathematical modelling of the combustion of a single wood particle. *Fuel Processing Technology*, 2006;87:169-175.
- [17] Prakash N, and Karunanithi T. Advances in modelling and simulation of biomass

pyrolysis. *Asian Journal of Scientific Research*, 2009;2(1):1-27.

- [18] Sadhukhan AK, Gupta P, and Saha RK. Modelling and experimental studies on pyrolysis of biomass particles. *Journal of Analytical and Applied Pyrolysis*, 2008;81:183-192.
- [19] Sadaka S. and Donald M. Johnson. Biomass combustion. *Agriculture and Natural Resources*.
- [20] Kiuru T. and Hyytiainen J. Review of current biocoal production technology.
- [21] Yao B. Yang, Vida N. Sharifi, Swithenbank J, Ma L, Leilani I. Darvell, Jenny M Jones, Pourkashanian M, and Williams L. Combustion of a single particle of biomass. *Energy & Fuels*, 2008;22:306-316.